S
FACULTY OF SCIENCE AND TECHNOLOGY

BACHELOR'S THESIS

Study programme / specialisation: Kjemi og miljø	**The *spring* semester, *2023*** **Open**
Author: Hanna Elisabeth Svendsen	*Hanna E. Svendsen* .... **(signature author)**
Supervisor at UiS: Sachin Maruti Chavan	
Thesis title: Adsorption remediation of perfluoroalkyl and polyfluoroalkyl substances (PFAS) from Water.	
Credits (ECTS): 20	
Keywords: MOF Zr-MOF-808-Ac PFAS Adsorption LC-MS	**Pages**: 47 **+ appendix**: 21 **Stavanger, *15.05.2023***

Abstract:

PFAS compounds are widely used in firefighting foams, non-stick pans, waterproof clothing, and many other things used in normal life. PFAS are carbon chains at least one or all hydrogens are substituted with a fluoride atom. The carbon and fluorine bindings are very strong making the PFAS difficult to remove from the environment. It has been reported that PFAS may lead to health effects for humans and animals, like cancer and birth defects. What makes this more dangerous is that it is nearly impossible to remove from water because they are very soluble in water. When it was discovered how dangerous the compounds are, shorter chains compounds were developed to substitute the longer chained compounds. These were supposed to be less dangerous to the environment. But it is now clear that the shorter chains may be as dangerous as the longer chains, and they may be more difficult to remove from the environment.

Reverse osmosis foam fractionation and adsorption on carbon-based materials are some techniques that are used to remove PFAS from water, but they are not as efficient as they should be. Therefore, a more effective technique that shows high efficiency is needed. Metal-organic frameworks are microporous crystalline, three-dimensional porous material. MOFs by virtue of their high surface area and specially designed pore functionality could adsorb PFAS on a higher scale and be a solution to the problem.

In this project synthesis of Zr-MOF-808-Ac was performed and characterized by XRD, TGA, N_2-sorption, SEM-EDS, and NMR to confirm the synthesis. Adsorption experiments were conducted with three different PFAS (PFOA, PFBS and PFBA) to examine the uptake of PFAS to MOF-808. LC-MS instrument was used to determine the concentration after the adsorption experiment.

The PXRD-characterizing indicated that the MOF-808 synthesis was successful, but the sample still contained a lot of unreacted residues solvent (precursors). The surface area for unwashed was 1455 m^2/g and for washed was 1603 m^2/g, this is lower than reported in literature, so the surface area is not optimal. This could be solved by optimizing the washing procedure. The quantitative analysis of the PFAS solution before and after the adsorption using the LC-MS instrument indicated a high uptake of PFOA and PFBA, but approximately no change in concentration of PFBS. This could be due to poor washing of MOF-808 or that MOF-808 don't have the ability to adsorb PFBS.

Acknowledgments:

Table of content

List of figures:

List of tables:

Abbreviations:

MOF – Metal organic framework

PFAS – Perfluoroalkyl and polyfluoroalkyl substances

PFOA – Perfluorooctanoic acid

PFBS – Perfluorobutanesulfonic acid

PFBA – Heptafluorobutyric acid

SEM-EDS – Scanning Electron Microscopy – Energy Dispersive X-ray spectroscopy

NMR – Nuclear Magnetic Resonance Spectroscopy

PXRD – Powder X-ray Diffraction analysis

TGA – Thermogravimetric Analysis

IUPAC - International Union of Pure and Applied Chemistry

BET – Brunauer-Emmett-Teller Theory

1. Introduction

1.1 PFAS

Environmental toxins are a big issue in today's society. They are dangerous to human health and the ecosystem. One of the most dangerous ones are Per- and polyfluoroalkyl substances (PFAS), synthetical components that are widely used today and has been since around the 1940s. PFAS are carbon chains where the hydrogens are being replaced with fluoride atoms. In perfluorinated substances, all the carbons are completely replaced by fluoride atoms. Polyfluorinated substances have at least one carbon remaining in one of the chains (bell, 2019). The bond between the carbon and fluorine atom is the strongest bond in organic chemistry. This makes the PFAS highly stable and difficult to break down (Pedersen, 2023). PFAS occur in the soil, in water and in the air. And can travel both in soil and with the air (Altarawneh, 2021).
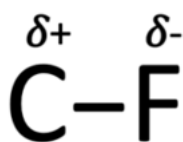
Figure 1-1. C-F bond partial charge presentation. (The Science of PFAS, 2021)

Non-stick pans, water resistant clothes and fire foam among other things where PFAS are used (Andreassen, 2023). PFAS remains unchanged in nature and therefore it exists in drinking water, in the air, in the soil, food, the packaging and in the things that the food is made in. Contaminates surface and ground water. The human body is also unable to metabolize it and will stay in the body for a long time. In the human body PFAS can affect the immune system, and -vaccines and can lead to various types of cancer. Some of them can lead to birth defects and have similar effects on plants and animals. At the time it exists around 10000 different types, and new types are made all the time. Because of the danger connected to PFAS, and how difficult it is to remove, new technology to remove the substances is important and relevant.

Some groups of PFAS can bioaccumulate in humans and animals and have been found in human blood and breast milk (*Perfluorerte stoffer (PFOS, PFOA og andre PFAS-er)*, n.d.). Exactly how dangerous the health effects of PFAs are unsure, but some of the known effects are cancer, hormone-oxidizing, and interfering with reproduction and the immune system. When the immune system is weakened vaccines will not be as effective as it is supposed to

be. In animal studies PFHxA has led to reduced weights and increased stillbirths. PFHxA also accumulates in plants and makes it easier for humans and animals to consume more of it. (*Perfluorerte stoffer (PFOS, PFOA og andre PFAS-er)*, n.d.). See table 1 for the health effects and use for a selection of PFAS.

Table 2-1. Different PFAS, where they have been used, their characteristics and health effects.

PFAS	Characteristics	Health effects	Use
PFOS	*Forever poison in water, accumulates easily in organisms and in food chains*	*Birth effects and is suspected to cause cancer. It's also dangerous to swallow and inhale.*	*Stain-resistant fabrics, fire-fighting foams, food packaging and surfactant in industrial processes*(PFOS and Groundwater, n.d.).
PFHxS	*Accumulates easily in organisms and in food chains*	*Hormone-disrupting and among other things, toxic to the liver and nervous system*	*Used in non-stick pans, in water-, grease- and stain-resistant things. PFHxS is also used in firefighting foams (jnelson, 2022).*
PFBS	*Affect the hormonesystem and reproduction in fish. Mobile in water and remains in water after cleaning.*	*Affects the hormonesystem and reproduction in humans.*	*4-C and introduced when PFOS got restrictions. PFBS have been used as surfactant in* industrial processes, on products like fabrics, carpets and paper like a water-resistant or stain-resistant coating (bell, 2019).
PFOA	*Accumulates very easily in organisms and in food chains*	*Birth defects and can cause cancer.*	*Has been used as processing aid and in fire-fighting foams* (Shen et al., 2023)
C9-C14 PFCA	*Accumulates very easily in organisms and in food chains*	*Birth defects and can cause cancer.*	*Used surfactant applications, and in the production of large molecules called fluorotelomers* (Canada, 2017).
PFHxA	*Mobile in water and remains after cleaning. May accumulate in plants.*	*Shown in animal studies to reduce birthweight and increased the number of stillbirths.*	*PFHxA is a breakdown product of other PFAS and have been used in carpets, and stain-resistant fabrics. Also used in manufacturing photographic film. Substitute for long-chained PFAS in consumer products* (US EPA CENTER FOR PUBLIC HEALTH & ENVIRONMENTAL ASSESSMENT & Kraft, n.d.).
HFPO-DA	*It does not break down in nature and is highly mobile in water. Studies have shown that the substance can cause irreversible and serious effects in rats.*	*Has caused cancerous tumors and liver damage in animal studies*	*Used as a substitute for PFOA in the production of fluoropolymers.*

Effects of PFAS on human health

Per- and polyfluorinated alkyl substances (PFAS) are a group of extremely persistent chemicals that are used in many consumer products. PFAS are used in products because they can, for example, increase oil and water repellence or resist high temperatures. Currently, there are more than 4 700 different PFAS that accumulate in people and the environment.

High certainty
Lower certainty

Developmental effects affecting the unborn child

Delayed mammary gland development

Reduced response to vaccines

Lower birth weight

Obesity

Early puberty onset

Increased miscarriage risk (i.e. pregnancy loss)

Low sperm count and mobility

Thyroid disease

Increased cholesterol levels

Breast cancer

Liver damage

Kidney cancer

Inflammatory bowel disease (ulcerative colitis)

Testicular cancer

Increased time to pregnancy

Pregnancy induced hypertension/pre-eclampsia (increased blood pressure)

Sources: US National Toxicology Program (2016); C8 Health Project Reports (2012); WHO IARC (2017); Barry et al. (2013); Fenton et al. (2009); and White et al. (2011) apud Emerging chemical risks in Europe — 'PFAS'.

*Figure 2-2. PFAS health effects on humans. (*Effects of PFAS on Human Health — European Environment Agency, *n.d.)*

Table 1-2. shows the levels of five different PFAS in the blood of grownups and children.

Table 1-3. (Haug et al., 2018b). Medianconcentrations of some PFAS in grownups and children blood.

	PFOS	PFOA	PFHxS	PFNA
Voksne	7,7 ng/mL	1,9 ng/mL	0,67 ng/mL	0,61 ng/mL
Barn	3,2 ng/mL	3,3 ng/mL	0,79 ng/mL	0,60 ng/mL

1.2 PFAS occurrence in the environment:

The use of PFAS in ski lubrication has been widely discussed in Norway the last years. PFAS makes the skis glide better, but it is hazardous to health for the people working with it. The fluor on the skis will affect the environment around where the skis are being used. This includes the animals living in the forest, and fish living in nearby lakes.

Measurements of PFAS shows that for the last few years it has been stable and have decreased. This may be because globally new restrictions are being placed on the use and handling of waste. But ways to remove them will still be important and relevant because these substances are "forever", because they don't go away naturally. So even if we stop using PFAS, it will still exist in the environment, and we can still get it in us through drinking water. Another problem is that when one type of PFAS is banned, new ones are made and used. Therefore some countries work on prohibiting alle types of PFAS (*All News - ECHA*, n.d.; *Forslag om å forby alle PFAS-er lanseres i Brussel - Miljødirektoratet*, n.d). See figure 3 for some values of PFAS in drinking water and wastewater in different countries in Europe.
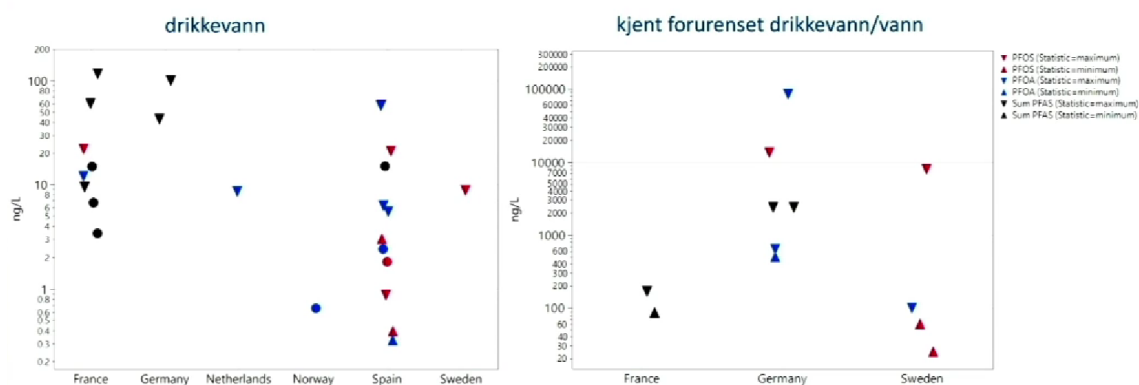

Figure 1-3. Values of PFAS in drinking water in some countries in Europe (Vann, 2022).

Shorter chains bioaccumulates less than longer, and therefore the last years it's been working on replacing the long chains with shorter chains that have the same qualities. But the PFAS are still not good for the environment and the shorter chains are more difficult to clean out

from water. Studies shows that many of the short chained PFAS have the same health effects as the long chains. This is a worry since they are more difficult to get rid of (Brendel et al., 2018; Renner, 2006). In Norway the limit for PFAS in drinking water is 100ng/l, but the water works are still supposed to try to decrease the amount of PFAS in the water that we will drink (Vann, 2022). PFAS is found in water in the whole country, but some groundwater and surface water has very high values(*Perfluorerte stoffer (PFOS, PFOA og andre PFAS-er)*, n.d.). This may come from leaks and often from places where fire foam containing PFAS has been used. The compositions of PFAS have changed over the years, and therefore it is possible to understand approximately when and where the leakage originating from. Other places in Norway where the values are higher than normal is around airports (often because of fire foam) and places where skis have been tested. The values are also higher around companies that produces PFAS or uses it in other ways. (*Perfluorerte stoffer (PFOS, PFOA og andre PFAS-er)*, n.d.)

The two most common PFAS are PFOA and PFOS, Figures under. PFOA and PFOS are phased out, but there are still other substances that are still produced. The values of them have gone down after measurements. PFOA is the PFAS with the highest concentration in the blood of adults in Norway (Haug et al., 2018a).

Figure 1-4. Structure of PFOA and PFOS (n.d.)
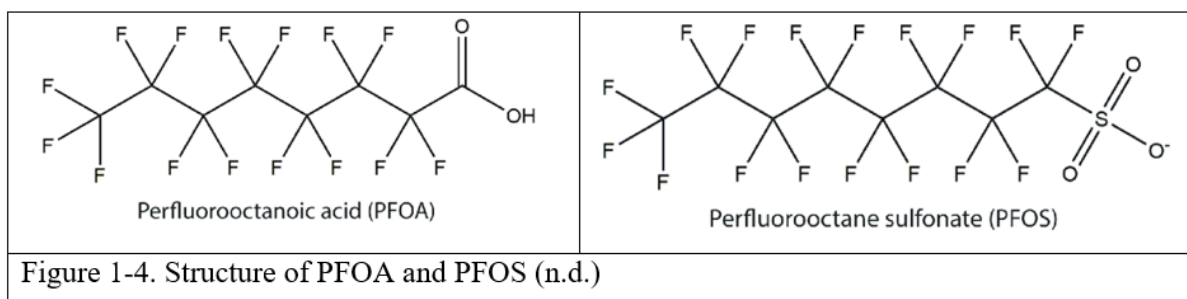
There are used different things like carbon-based materials, ion exchange resins, biomaterials and polymer to remove PFAS from wastewater (Karbassiyazdi et al., 2023). None of these are optimal methods since it's difficult to use in a bigger scale. Metal organic frameworks (MOFs) are components that can easily be created with the components that gives the wanted structure. The 3D structure and stability make the MOFs so special and relevant in adsorption work. This study will be in two parts. The first part will be about establishing a way to quantify PFAS in water and the second part will be about adsorbing PFAS to MOF-808(Cserbik et al., 2023).

2. Literature review

2.1 Technology to remove PFAS from water

The technologies that are used to PFAS from water now is reverse osmosis where the water is pushed through a membrane and in theory the PFAS will be stopped because it's not small enough to get through the pores in the membrane. In reality most of the PFAS will also go through the membrane and the water will still be full of PFAS.

Another technique is to use carbon-based materials such as filters. Also, here the water will get through and the PFAS will be left in the filters. Ion exchange is another technique to remove PFAS where PFAS ions is exchanged with another ionic substance (*PFAS Removal by Ion Exchange Resins*, n.d.) Covalent organic frameworks (COFs) and Zeolitic imidazolate frameworks (ZIFs) can be used to adsorb PFAS, but some problems with these techniques are that some of the work great on longer chains, but they can't trap the shorter chains (FitzGerald et al., 2022; *PFAS and Home Treatment of Water - MN Dept. of Health*, n.d.).

2.2 Adsorption

Adsorption is a separation process where molecules or ions are transferred from a gas, or liquid to surface of a solid or liquid. In this project PFAS from liquid media water will adsorb onto MOF-808. Therefore, the process is called liquid-phase adsorption process, the molecules are transferred from a fluid bulk to a solid surface. The process is reversible and that is called desorption. The molecules that are transferred are called the adsorbate and the solid that adsorb the molecules on its surface is called the adsorbent. The space uptake by the adsorbate is called the adsorption space. Particles used for adsorption usually has small pores and a very high surface area.

The solid-liquid process can be parted in three steps. In the first step the adsorbate is transferred from the liquid bulk by diffusion to the solid external surface. Then the equilibrium between the liquid phases and the adsorbent.

In step two the adsorbate will transferred to the adsorbed phase and the pores of the adsorbent. In the third and last step the adsorption of the adsorbate is happening at the adsorbent's pores. The adsorbents surface has many pores and channels, depending on the type of adsorbent, that the molecules will attach to with diffusion (Thommes et al., 2015).

2.3 MOF structure and Zr- MOF – 808-Ac

Metal organic-framework (MOFs) have been popular to research the last two decades because of its high potential for wide areas of use. Metal organic-framework (MOFs) are porous hybrid materials made of metal ions or metal-oxo cluster connected with organic material as bridges between the ions. These bridges between the ions creates a lattice structure (Farha et al., 2010). The interests in MOFs have increased the last few years because of the modular nature of the framework that allows the designing of MOFs for a targeted application. The lattice structure gives the MOFs a large specific surface area and the pores sizes can be designed after the area of use with different inorganic and organic building blocks (Chang et al., 2022). For adsorption in liquid media, one needs a MOF that is chemically stable. The zirconium MOFs with carboxylate linkers forms a good choice. Due to the strong Zr-O bond, these MOFs are chemically highly stable. Besides chemical stability, Zr-MOF also shows high thermal and mechanical stability (Aunan et al., 2021) (Chang et al., 2022).
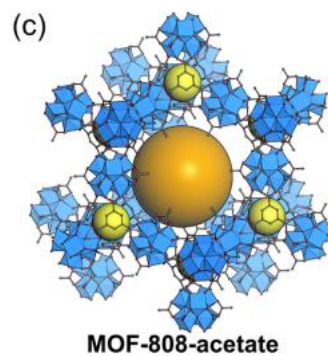

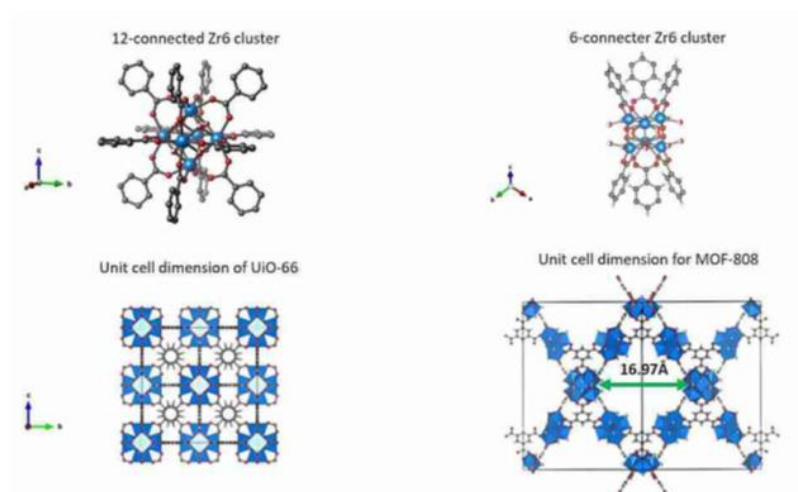*Figure 2-1. Structure of Zr-MOF-808-Ac (Aunan et al., 2021)*

Figure 2-2. Structures of UiO-66 and MOF-808. See that MOF-808 is a 6-connecter Zr6 cluster and UiO-66 is a 12-connected Zr6 cluster.

The Yaghi group was the first to describe zirconium-based MOFs in 2014 (ref. J. Am. Chem. Soc. 2014, 136, 4369−4381.) MOF-808 is based on a hexanuclear Zr-oxo cluster coordinated by only six tritopic linkers (trimesic acid). These forms a cage with tetrahedral shape. Guest molecules can adsorb because of the ligand position. The largest pore has a diameter of about 17 Å. The large pore size, chemical stability and accessible pores makes MOF-808 promising for PFAS adsorption (Aunan et al., 2021).

2.4 LC-MS

Liquid chromatography–mass spectrometry (LC-MS) is a way to analyze the concentration of different compounds. The MS part will make ions and analyze them. It can be used to decide the unknown concentration of different compounds. In this project the LC-MS instrument will be used to decide the concentration of PFAS before and after adsorption (*Fast and High-Resolution LC-MS Separation of PFAS*, n.d.)(Øiestad, 2018).

2.5 PFAS in this project

In this project/thesis MOF- 808 will be used to adsorb PFOA (Perfluorooctanoic acid), Perfluorobutanesulfonic acid (PFBS) and Heptafluorobutyric acid (PFBA).
The PFAS substances were chosen based on the numbers of carbons in the chain and their functional groups to examine how these properties will affect the adsorption. All of them are soluble in water, but in different manner. PFBS was chosen to examine the effect of the sulfonyl group. PFOA was chosen as a "longer" short chained substance. PFBA was chose as an example of a "shorter" alternative.
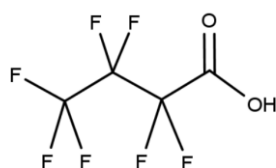
Figure 2-3. PFOA structure (Kolesnik, 2020)

Figure 2-4.PFBS structure («Perfluorbutansulfonsäure», 2021)
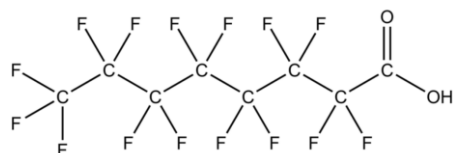
*Figure 2-5. PFBA structure (*Chemical Structure of Perfluorooctanoic Acid (PFOA)*, n.d.)*
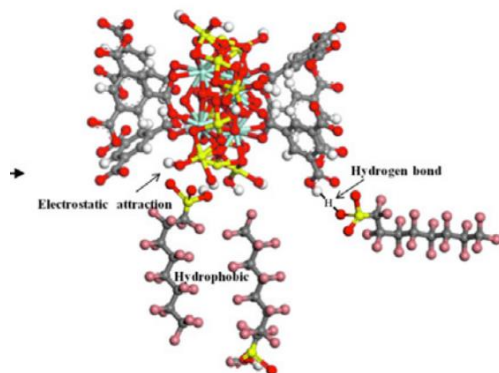
PFOS adsorbed on MOF-808

Figur 2-6. Structure of PFOS adsorbed onto MOF-808(Chang et al., 2022)

2.6 Thesis scope

This study is divided into two. The first part is to establish a method for quantitative analysis of PFAS in water at UiS. After the method is established, the aim is to investigate the effectiveness of MOF-808 in the adsorption removal of PFAS.

The motivation for this project is to find an effective way to remove PFAS from water because of all the consequences they have on human health and the environment. In addition, it is unclear how dangerous the molecules are, and this makes it even more important to find a solution to the problem. The solution should be able to remove both long and short chained PFAS and should not be harmful to the environment.

Adsorption was chosen as a technique because it's an effective and cheap method to separate molecules from water. The technique can also be scaled up if the project is successful. MOF was chosen as adsorbate because of its adjustable pore sizes and its stability in water.

3. Materials and method

3.1 Materials

Table 2 shows all chemicals used. Zirconium (IV) oxychloride octahydrate, Trimesic acid, acetic acid, Perfluorooctanoic acid, Nonafluoro-1-butanesulfonic Acid and Heptafluorobutyric acid.

Table 4-1. Chemicals used in experiments.

Application	Chemicals	Common name	Producer	Purity
Metal source	$ZrOCl_2*8H_2O$	*Zirconium (IV) oxychloride octahydrate*	*Sigma Aldrich*	*98%*
Linker	H_3BTC	*Trimesic acid*	*Sigma Aldrich*	*95%*
Modulator	CH_3COOH	*Acetic acid*	*Tokyo Chemical Industry*	*98%*
PFOA	*C8HF15O2*	*Perfluorooctanoic acid*	*Sigma-Aldrich*	*95%*
PFBS	$C_4HF_9O_3S$	*Nonafluoro-1-butanesulfonic Acid*	*TGI*	*>98.9%*
PFBA	$C_4HF_7O_2$	*Heptafluorobutyric acid*	*TGI*	*>98.0%*

3.1.1 Procedure Synthesis of Zr-MOF-808-Ac

(Aunan et al., 2021) was used with water to get a green synthesis.

Chemicals required: Zirconium (IV) oxychloride octahydrate ($ZrOCl_2.8H_2O$, 98%, Sigma Aldrich), Trimesic Acid (H_3BTC, 95%, Sigma Aldrich), Water and acetic acid ($C_7H_6O_4$, 98%, Tokyo Chemical Industry).

Zirconium (IV) oxychloride octahydrate (10.5 g) was added to a round bottom flask and dissolved in distilled water (35.25 ml). Acetic acid (93.17 ml) was added to the solution and stirred. When obtained clear solution trimesic acid (2.348 g was added). The solution was stirred at 95 °C for 72 hours under reflux conditions. The product was poured into a centrifuge tube and centrifuged at 4000 RPM in Eppendorf Centrifuge 5804 R for 10 minutes. The solid product was washed 5 times with distilled water and dried in an oven for 22 hours at 60 °C. The product was ground and weighed(Aunan et al., 2021).

Table 3-2. Synthesis table for Zr-MOF-808-Ac.

	ZrOCl$_2$*8H$_2$O	Trimesic Acid	Acetic Acid	H$_2$O
Mm(g/mol)	322.25	210.14	60	18.02
Molar Eqv.	1	0.33	50	60
Mmol	32.58	11	1629	1955
Density	-	-	1.05	1.00
Amt used (g or ml)	10.5g	2.348g	93.17ml	35.25ml

Figure 3-1. Synthesis of Zr-MOF-808-Ac. Experimental setup.

3.1.2 Procedure for washing:

After synthesis the product was centrifuged and washed five times with water. Then dried in the oven for over- night. Then the sample was ground. The product was analyzed with TGA, XRD and nitrogen adsorption. 1 g of the product was washed 3 times with distilled water and 2 times with acetone and put in the oven overnight. Before each centrifuging the sample was shaken very well in the water or acetone. The same analyses were done on the washed sample to look at the difference.
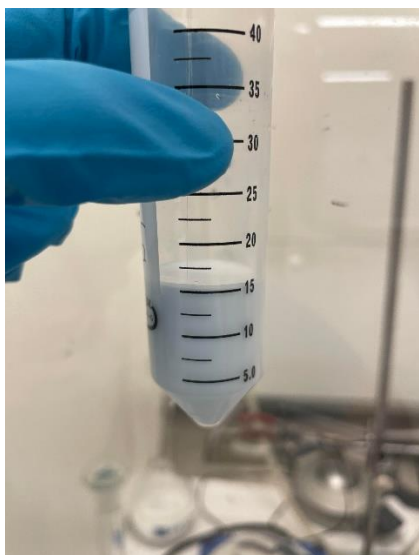
Figure 3-2. Zr-MOF-808-Ac product after synthesis before centrifugation and drying.

3.2 Methods:

3.2.1 Powder x-ray diffraction (PXRD):

Theory:

With XRD the purity, structure of the sample and the composition of impurities present in the sample can be determined in a nondestructive way. The XRD sends out X-rays source. When X-rays hits crystals they will diffract in a characteristic pattern for each crystal. In XRD the pattern is obtained from the pattern of the powder, instead of a single crystal. The pattern is intensity against the angle of the detector, that is 2 theta degrees. The X-rays will be partially scattered when it hits a crystal layer, and that way it will create a pattern. To get this pattern and for the x-rays to diffract the powder needs to be crystalline and the spacing between each atom layer needs to be approximately the same as the radiation wavelength. If the rays are diffracted by two different layers are in phase, there will occur constructive interference. Constructive interference will give diffraction peaks. Destructive interference occurs when the layers are not in phase and there will be no diffraction peak in the XRD plot. Therefore, only crystalline compounds will show in the plot, and amorphous compounds will not show diffraction peaks. The higher and more intense peaks, the purer and more crystalline compound.

Diffraction peaks only occur if Braggs-law is satisfied:

$$2dsin\theta = n\lambda \qquad \text{Eq. 1}$$

Where θ is the angle of incidence of the X-ray, n is an integer, λ is the wavelength and d is the spacing between the atom layers (Holder & Schaak, 2019; *Powder X-Ray Diffraction*, 2013).

Procedure:

With mortar and pestle the samples were ground to a fine powder. To produce the most accurate and quality results, powder plates should be used for analysis, but this requires about 0.2-0.3 g of the compound. Samples with lower quantity than 0,2 g can be analyzed on a slurry plate instead. The samples are made into a slurry by adding ethyl alcohol dropwise into the plate (Ø 51.5mm, Ø 24.55mm Si crystal), then the slurry plates were left until dry. The samples were placed into the D8 Advance-Bruker XRD and scanned for a long time and 2°-70° for short a time. It took 11 minutes per sample for shorter times, and around 15 minutes for longer runs. The divergence slit was 0,6mm and with 0.01 increment. In this project all the analysis were done using the slurry plates and none on powder plates due to the low quantity of some samples and the wish for consistent results. The results were converted to XY-files and plotted with QtiPlot.

Figure 3-3. XRD-instrument.

3.2.2 Thermogravimetric analysis (TGA):

Theory:

Thermal analysis (TA) is another method to verify the quality of the sample. Measurement of properties in a compound as the temperature is changed. The properties can be mass, volume, chemical compositions, and magnetism. The atmosphere can also be changed so the analysis can be done in a vacuum, inert atmosphere, or synthetic gas mixtures. In TGA the property of mass is measured as the temperature is changed. From a TGA plot, the amount of solvent and unreacted solvents can be extracted. The first flat point/step/plateau in weight% can indicate the solvent leaving the sample, the next flat point indicates that unreacted linkers are leaving. Also shows modulator the loss of the modulator. The weight loss comes from evaporation or breaking of bonds when the temperature rises. The first step is also important to choose the activation temperature for nitrogen adsorption because that is when the solvent and moisture leaves the pores (Wei et al., 2017).

Procedure:

Approximately 10-25 mg of the sample was weighted and placed in an alumina oxide crucible, then weighted again to get the total before analysis. Then the sample was put in the machine and the temperature increased stepwise from 25°C up to the desired temperature (Here: 800°C). The sample is continuously weighted in a controlled environment. The heating rate used is 10°C per minute, synthetic air that purges the environment at a rate of 20 ml per minute. Mettler Toledo TGA/DSC 3+ stare system was used, and synthetic air as a purge gas to control the analysis environment.

Figure 3-4. TGA-instrument.

3.2.3 Nitrogen-sorption (BET):

Theory:

Nitrogen adsorptions were performed to decide the porosity and the pore size of the sample, and to understand the surface of the sample. Nitrogen adsorption is used to get the adsorption isotherm and BET theory is used to analyze it. Other adsorbates like CO_2 can be used, but nitrogen is the most common to use. The nitrogen adsorbed is plotted against the relative pressure and is repeatedly measured. The plot illustrates various pressures of gas in the sample cell because of adsorption and desorption. Further the computer software will calculate the surface area and pore size. The result is called an isotherm, see adsorption theory. The isotherm indicates which types of pores the surface of the sample contains. The desorption curve is also calculated through the data.

The Brunauer, Emmet and Teller (BET) equation were used to determine the surface area of the washed and unwashed samples from the nitrogen adsorption isotherm. BET is the most common method to describe specific surface areas.

$$\frac{1}{W\left(\left(\frac{P_0}{P}\right)-1\right)} = \frac{1}{W_m * C} + \frac{C-1}{W_m * C} * \left(\frac{P}{P_0}\right) \quad Eq.\,2$$

Where:

W is the weight of nitrogen adsorbed, P/P_0 is the relative pressure. Wm is the weight of weight of the adsorbate as monolayer, and C is the BET constant {Citation}.

To calculate the total specific surface and the specific surface area the slope, intercept, Wm and C (BET constant is required):

Slope (s) and intercept (i):

$$s = \frac{C - 1}{W_m * C} \quad Eq.3$$

$$i = \frac{1}{W_m * C} \quad Eq.4$$

Wm (Weight of monolayer):

$$W_m = \frac{1}{s + i} \quad Eq.5$$

C (BET constant):

$$C = 1 + \frac{slope}{intercept} \quad Eq.6$$

These equations can be used to calculate the BET surface area:

$$BET\ surface\ area = \frac{NaPV_m}{RT} * \sigma_0 \quad Eq.7$$

Total pore volume can be calculated from Eq. 9:

$$V_t = \frac{n_m}{b} \quad Eq.8$$

V_t is the total pore volume in cm^3/g, n_m is the adsorption capacity at 0.9 relative pressure and b is the liquid and gas ratio for nitrogen with the value of 694.

The surface can have microporous pores (diameter <2nm), mesoporous pores (diameter 2-50nm) and macropores (diameter >50nm). The pore size can be understood in terms of isotherm. IUPAC has decided about 6 types of isotherms for gas-solid eq. that can describe the pore size. Type 1: Follows the Langmuir theory and monolayer adsorption. Indicates

16

microporous pores, when filled, leaves little or no external surface available for adsorption. Langmuir Equation describes microporous material exhibiting type 1 Isotherms. But assumes the adsorption is limited to one monolayer. Type 2: often describes the adsorption on nonporous powders or surfaces with pores with a longer diameter than the micropores. The inflection point is reached when the first monolayer is adsorbed. Type 3: is obtained when all layers are present at the same time, illustrated in an almost exponential graph. A type 4 isotherm indicates an adsorbent with pores from 1,5 to 100nm. When the experiment is reaching higher pressures, the graph will show a higher uptake of adsorbate because the pores become full. The point of inflecting is reached when the first monolayer is close to completion. Type 5 has a small adsorbate-adsorbent interaction potential, like type 3. The pores have a range from 1,5 to 100nm (Chang et al., 2022) (*Adsorption Isotherm and Its Types - Chemistry Notes*, n.d.).
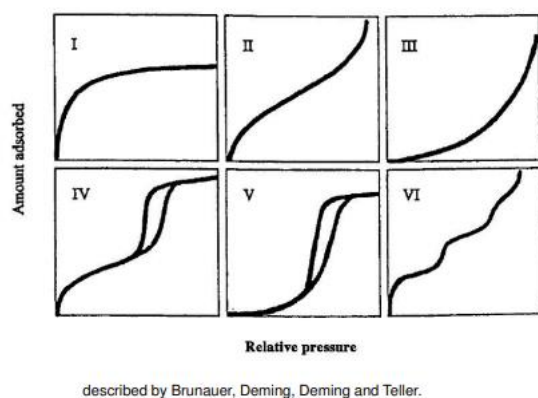

described by Brunauer, Deming, Deming and Teller.

Figure 3-5. IUPAC isotherms.

Procedure:

Micromeritics TriStar II Plus was used to perform nitrogen adsorption. Empty cell and rubber were measured, and the weight was noted down. Approximately 0.15 to 0.17g of sample was measured and added to the cell. Then the cell with sample and rubber were measured again. The quantity was important, so it was enough sample left after purification. The samples were degassed at 180 degrees for 3 hours under a vacuum to ensure clean and empty pores and surface. The degassing could also have been done under a flow of dry, inert gas. The activated samples were measured again. See table for weight before and after activation. Further the cells was inserted into the instrument and the experiment were performed at 77 K. Liquid nitrogen was used to cool down the examined solid. The files were converted into xls and plotted using excel.
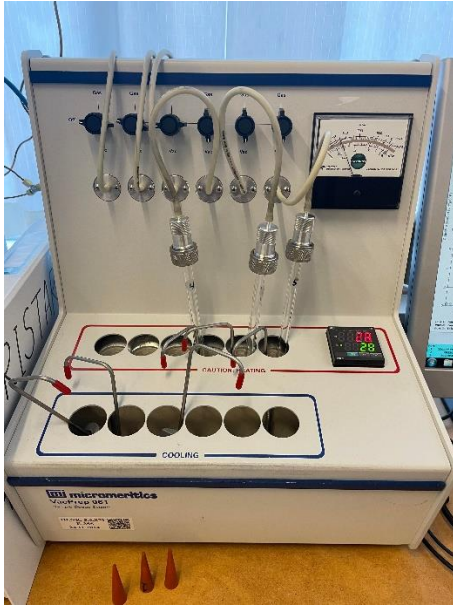
Figure 3-6

Figure 3-7

3.2.4 Batch adsorption:

The isotherm of adsorption describes the adsorption capacity together with the equilibrium concentration of the adsorbate. This gives a vision of the maximum adsorption capacity of the adsorbent and the adsorbate. The amount adsorbed can be calculated through the adsorption capacity equation:

$$q = \frac{(C_0 - C_e) * V}{m} \quad Eq.\,10$$

Where C_0 and C_e are the concentration of the adsorbent (PFAS) before and after adsorption. M is the mass of the adsorbent (g). The V is the volume of the solution (Chang et al., 2022).

Procedure:

Solutions of 20mg/L of each PFAS were prepared in a 250mL volumetric flask using 0.005g of PFOA, 0.00276 mL (2.76 µL) of PFBS and 0.003039 ml (3.04µL) of PFBA. Samples with concentrations of 10, 6, 2, 0.8, 0.5, and 0.2 mg/L were diluted from the 20 mg/L solution.

Experiment 1: 0.5g MOF was activated at 150°C for 2 hours. 0.05g was added to 25 ml of 1 mg/100ml of each PFAS.

Experiment 2: 1g MOF and what was left after activation of batch 1 were activated at 150°C for 2 hours. 0.05g MOF was added to 25 ml of 10, 6, 2, 0.8, 0.5, and 0.2 mg/L of each PFAS. PFBA only had the 10, 6, 2 and 0.8 mg/L concentrations because of a measuring failure of activated MOF. The sample with PFBS at 10 mg/L did not have a stirring magnet, and this may also have affected the result.

Both experiments were put on stirring at 30°C for 72 hours. The samples were cooled down and centrifuged at 4000 RPM for 10 minutes. The solids were put in the oven overnight at 60°C and the liquid was filtrated using a syringe and a 0.22 µm syringe-filter. Solids were analyzed in XRD to examine if the structure were still intact. The solution was analyzed in an LC-MS instrument for concentration after adsorption.

Figure 3-8. Adsorption experiment.

3.2.5 Scanning Electron Microscopy (SEM-EDS):

Theory:

Scanning electron microscopy – Energy dispersive spectroscopy (SEM-EDS) is an effective method to analyze organic and inorganic compounds from nanometer to micrometer scale. It is a nondestructive analytical method to understand the particle morphology and composition of a compound. It gives very precise pictures of many different compounds. Together SEM and EDS give information on the composition of the materials. The instrument will send out electrons that will emit x-rays that are specific for each element that is present in the sample. Samples were analyzed with Gemini SUPRA 35VP (ZEISS) (Carl Zeiss, Jena, Germany) with EDAX energy dispersive Xray spectroscopy (EDS) (*SEM/EDS Analysis | RTI Laboratories*, 2016).

Procedure:

The samples were finely grounded to a fine powder and put on the sample holders with the help of carbon tape to reduce the height differences and get a smooth surface. Further, the samples were put in the instrument and examined with SEM under a magnification of 500-5000. 3-4 spots were chosen on each sample and analyzed for the composition of the sample using the EDS. The results were files with pictures of the sample, graphs and tables that visualized the composition of the samples.
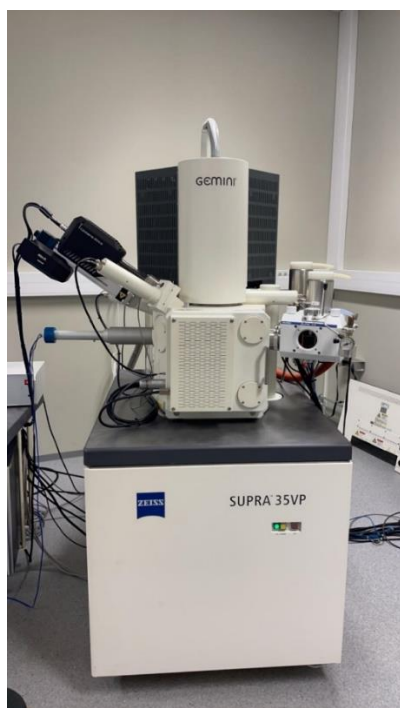

Figure 3-9. Gemini SUPRA 35VP (ZEISS) (Carl Zeiss, Jena, Germany) with EDAX energy dispersive Xray spectroscopy (EDS). SEM-EDS intstrument.

3.2.6 Liquid Chromatography-Mass Spectrometry:

Theory:

An analytical technique that combines liquid chromatography with mass spectrometry. The liquid chromatography (LC) part separates the samples, and the mass spectrometry (MS) part will create and detect charged ions. The MS part ionizes the sample and fragments it. Then the mass is calculated and divided by the charge meaning that the ions are being weighted. Therefore, it can be used to find the molecular weight structure and quantity of compounds. Can be used on samples that don't work in GC/MS. This is because in LC-MS no heat or little heat will impart to the analyte. Therefore LC-MS suits to analyze large, polar, ionic, thermally unstable and involatile compounds. And it allows MS analysis of non-volatile, thermally labile, or charged molecules (Chemyx, 2017) .

Procedure:

An LC-MS machine was used to establish a method for quantitative analysis of PFAS in water at UiS. The calibration curves were made with eight points from 0.0003 mg/L to 0.2 mg/L. first it was made a 20 mg/L solution in a 250 ml volumetric flask for each of the PFAS. The 20 mg/L solution was diluted to 5 ml of 15 mg/L, 10 mg/L, 5 mg/L and 3 mg/L. These were further diluted to 0.0003 mg/L, 0.001 mg/L, 0.002 mg/L, 0.03 mg/L, 0.05 mg/L, 0.1 mg/L, 0.15 mg/L and 0.20 mg/L. The samples were made to make the calibration curve for each PFAS. There were made three blank samples for every analysis. The vials with the samples were put on the sample holder and into the instrument before the instrument was started. See the Appendix for the procedure for starting the instrument.

Figure 3-10. LC-MS instrument.

3.2.7 H-Nmr:

Theory and procedure:

NMR was used to analyze the loading of functional groups in MOF-808-acetate. The instrument used was Jeol 400Hz NMR Spectrometer. 20 mg of MOF-808 (washed and unwashed) were weighted and added to a centrifuge tube together with 1 M NaOH in D_2O. The tubes were shaken on an IKA MS basic shaker, before being stored for 24 hours. It was stored to make sure the organic compounds were out of the pores and that the inorganic component was gathered at the bottom of the centrifuge tubes. The samples were centrifuged with Centrifuge 5804 R from Eppendorf after 24 hours to separate the suspension. The suspension was transferred to the NMR tubes by a glass pipette for analysis. The data were plotted from the results.

Figure 3-11. Jeol 400Hz NMR Spectrometer, NMR-instrument.

4. Results and discussion

Zr-MOF-808-Ac was synthesized, washed, and dried. Then the sample was characterized by TGA, XRD, N_2-adsorption, H-NMR and SEM-EDS to understand the crystallinity, pore size and specific area. Then 1 g of the sample was washed 3 times with water and 2 times with acetone to clean the product properly. The same experiments were done on the washed sample. Then the unwashed product was used in the adsorption of PFOA, PFBS and PFBA. MOF-808 was again tested for crystallinity after the adsorption to examine if the structure

was still intact after adsorption. It was made a calibration curve for each PFAS with a LC-MS machine. This way the concentration could be checked before and after adsorption to understand if and how much PFAS was adsorbed by MOF-808. This section presents the results of the characterizing of MOF-808 (washed and unwashed) and the adsorption experiments.

4.1 MOF-808 synthesis:

The theoretical yield was calculated and compared to the experimental yield to understand if the sample contains a lot of water and need more drying, or to understand if reactants has been lost through the synthesis. The solution turned white after reaching the temperature 95°C. After centrifugation and drying in oven the sample was a white powder. The calculations below shows that the experimental yield is higher than the calculated theoretical yield, this could be related to unreacted modulators/linkers or/and not dry enough product. The synthesis was followed by the procedure reported by (Aunan et al., 2021).

The reaction happening during the synthesis (used for mol relations in calculations):

$$6\ ZrOCl_2.8H_2O + 6\ CH_3COOH + 2\ H_3BTC \longrightarrow [Zr_6O_4(OH)_4](BTC)_2(CH_3COO)_6]Cl_x$$
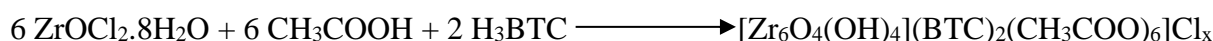
Calculations for theoretical yield and percent yield:

Calculation for mmol:

$$Amt\ of\ chemical\ used\ (g) * (\frac{1\ mol\ of\ chemical}{mass\ of\ chemical\ (g)} * \left(\frac{1000\ mmol}{1\ mol}\right)$$
$$= chemical\ in\ mmol$$

ZrOCl$_2$*8H$_2$O amount used = 10.5g

Theoretical yield:

$$Amt\ taken * 98\%\ g\ ZrOCl * 8H_2O * \left(\frac{1\ mol\ ZrOCl_2 * 8H_2O}{322.25g\ ZrOCl_2 * 8H_2O}\right) * \left(\frac{1mol\ product}{6mol\ ZrOCl_2 * 8H_2O}\right)$$
$$* \left(\frac{1447,76g\ product}{1mol\ product}\right) = \ g\ og\ product$$

Theoretical yield: 7.7g

Actual yield: 10.7970g

$$Percent\ yield = \frac{Actual\ Yield}{Theoretical\ yield} * 100\% = \frac{10.7970}{7.7} = 140\%$$

The experimental yield was 10.7970, that is 140% yield. This indicates that the sample contains a lot of water from the synthesis and the washing and drying performed was not successful.

Table 5-1.

	ZrOCl$_2$·8H$_2$O	Trimesic acid	Acetic acid	H$_2$O
Molar mass (g/mol)	322.25	210.14	60.052	18.02
Molar Eqv.	1	0.33	50	60
Mmol	32	11	1629	1956
Density (g/ml)	-	-	1.05	1.00
Amt used in synthesis	10.5 g	2.348 g	93.17 ml	35.25 ml

4.2 XRD:

Figure 7 shows PXRD patterns of MOF-808 unwashed (as-asynthesised) and MOF-808 after washing with water and acetone. The washed sample was around 1g and XRD with powder plates required a lot of sample. The samples were therefore done on slurry plates due to the low amount of the washed sample. The unwashed sample was therefore also measured on slurry to get comparable results. Both patterns show similar diffraction patterns.

The patterns are compaired to make sure that the structure is still intact after washing. The samples show diffraction points at the same 2 thetas, though a difference in intensity. The washed sample high intensity and a very low background than the unwashed sample.

This is because the water removes unreacted precursor residues leaving the high purity MOF. The difference in intensity can be because the washed sample is more pure and indicates higher crystallinity.
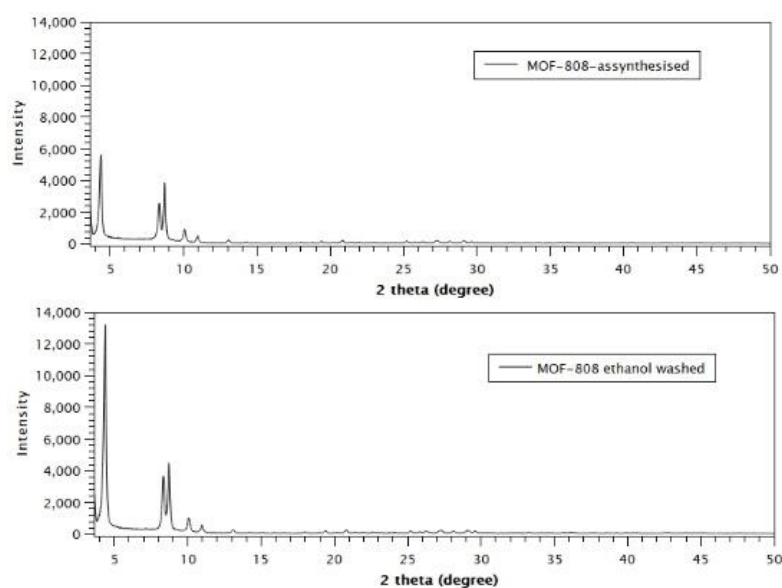
Figure 4-1. XRD plot of unwashed MOF-808 (above) and MOF-808 washed with ethanol (under).

To confirm the synthesis of MOF-808 the PXRD pattern of MOF-808-washed with water and acetone is compared with the simulated PXRD pattern (Figure. 8) The simulated pattern is obtained and downloaded from cif file from Cambridge Crystallographic Data Centre. The simulated pattern and the pattern for the washed sample show diffraction points at very similar points. This indicates that the synthesis of MOF-808 was successful and the results after the slurry plate are reliable.
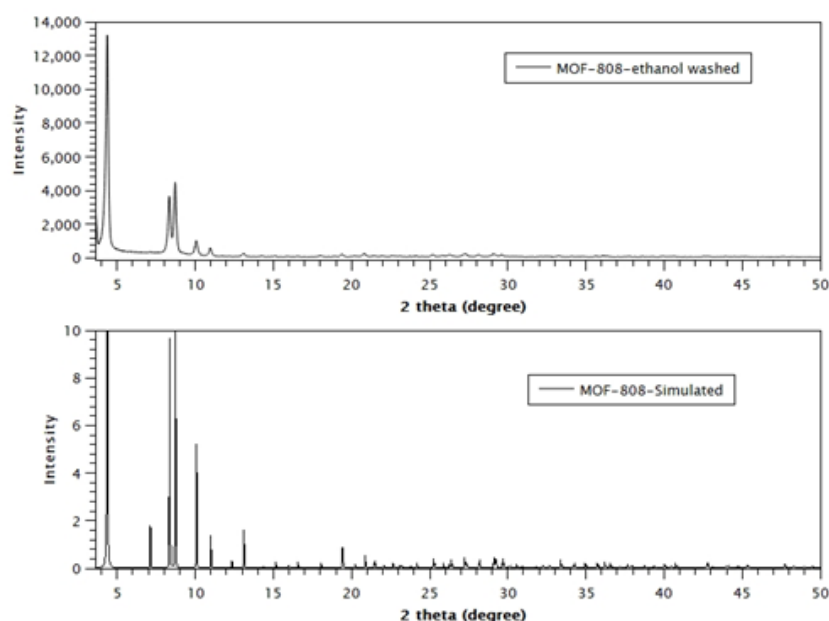
Figure 4-2. Cif- file downloaded from CIF file from Cambridge crystallographic Data Centre. Shows similarities in diffraction points.

4.3 TGA:

TGA was done to understand the weight loss due to temperature changes. Figure 9 shows the TGA plot for unwashed and washed Zr-MOF-808-Ac and the assumed decomposition. The first decomposition step indicates the loss of unreacted modulators and other solvents that were physisorbed in the pores. The second step is the de-hydroxylation of the zirconium nodes, meaning that the heating makes it lose -OH groups formed as a water molecule: $Zr_6O_4(OH_4) \rightarrow Zr_6O_6 + 2H_2O$. The third and fourth steps indicate the decomposition of MOF with the combustion of the modulator and linker. The steps are approximately marked by lines in figure 9 and are indicated by the flat plateaus. The red curve is the unwashed sample, and the black is the washed sample. When comparing the two curves they look quite similar with plateaus at approximately the same places. The only big difference is the curve down to the first step where the unwashed has a higher mass loss. This indicates that the washing has worked, and it is less unreacted modulators and solvent in the pores.

The theoretical calculation for each decomposition step can be calculated by dividing the molar mass of each decomposition by $6*ZrO_2$ and multiplying by 100 to get the percentage:

$Zr_6O_6BTC_2$ weight%:

$$\frac{MolarMass(Zr_6O_6BTC_2)}{6 * \text{MolarMass}(ZrO_2)} * 100\% = \frac{\frac{1057,57g}{mol}}{6 * \frac{123,218g}{mol}} * 100\% = 143\%$$

Weight loss linker: 143% - 100% = <u>43%</u>

$Zr_6O_6BTC_2(CH_3COO)_6$ weight%:

$$\frac{MolarMass(Zr_6O_6BTC_2(CH_3COO)_6)}{6 * \text{MolarMass}(ZrO_2)} * 100\% = \frac{\frac{1411.82g}{mol}}{6 * \frac{123,218g}{mol}} * 100\% = 191\%$$

Weight loss modulator: 191% - 143% = <u>48%</u>

$Zr_6(O)_4(OH)_4BTC_2(CH_3COO)_6$ weight%:

$$\frac{Mm(Zr_6O_4(OH)_4BTC_2(CH_3COO)_6)}{(6 * Mm(ZrO_2)} * 100\% = \frac{\frac{1447,87g}{mol}}{6 * \frac{123,218g}{mol}} * 100\% = 196\%$$

Weight loss de-hydroxylation of Zr-nodes: 196%-191% = <u>5%</u>

The theoretical and experimental decomposition steps can be compared to find missing linker defects. Figure 4-3 shows that the first experimental (120%) step is higher than the calculated (48%). This shows that it's a lot of unreacted modulators and solvents in the sample. The graph for the washed sample shows a very small first step (19%), indicating that the unreacted modulators and solvents have been washed away and that the sample is cleaner after washing. Comparing the unwashed and washed graph with the rest of the theoretical steps, they look very alike. This indicates that the MOF-808 sample has a high quality.
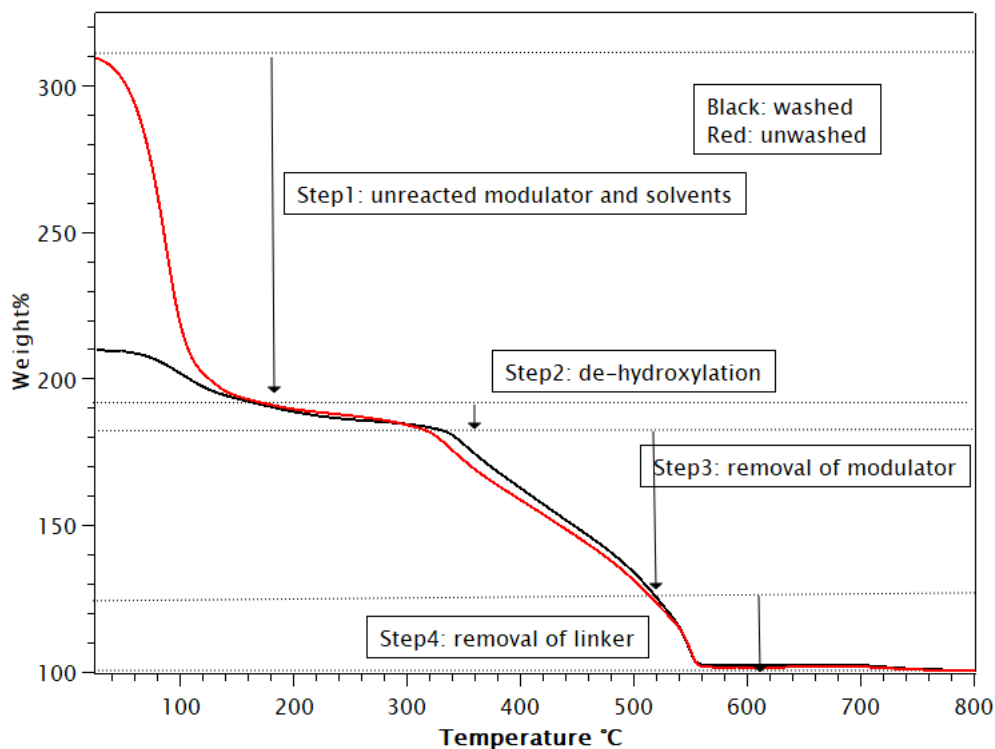
Figure 4-3. TGA for unwashed and washed MOF-808

4.4 N$_2$ sorption at 77k:

Figure 4-5 shows nitrogen adsorption (filled circles) and the desorption isotherms (not-fillet circles) of MOF-808-acetate after degassing for 3 hours at 160 °C and N$_2$-sorption at 77K. In the graph it can be observed first a linear step that indicates micropores (<2nm) before a plateau before going linear again. MOF-808 has two different kinds of pores, one bigger and one smaller. The BET plot, figure 4-6, shows two steps that is slightly deviating from type I isotherm, and this indicates that two different size micropores are present are present. The surface area was calculated to 1455 m^2/g. This area is much smaller than what is written in literature, were it is calculated to 1946 m^2/g (Aunan et al., 2021).
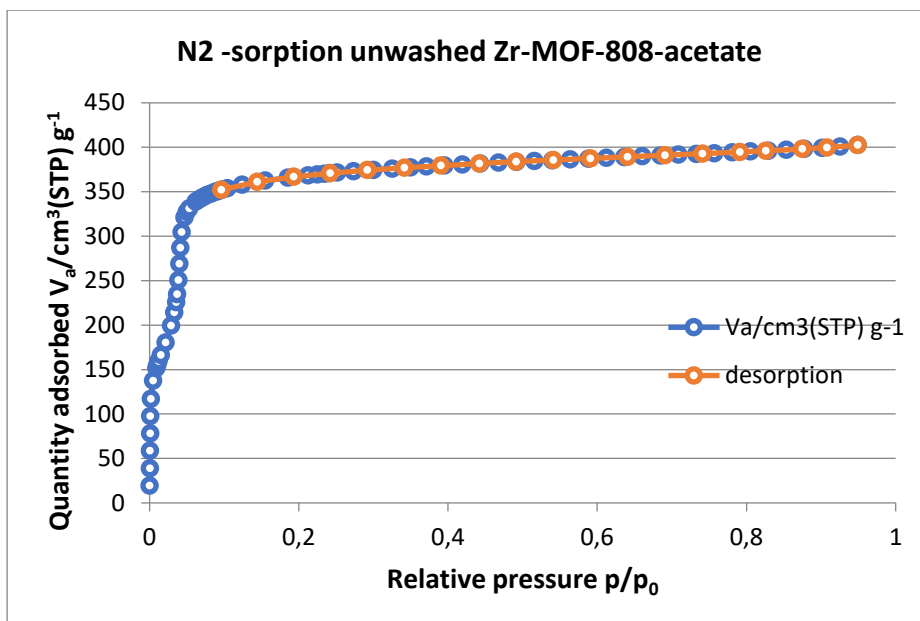
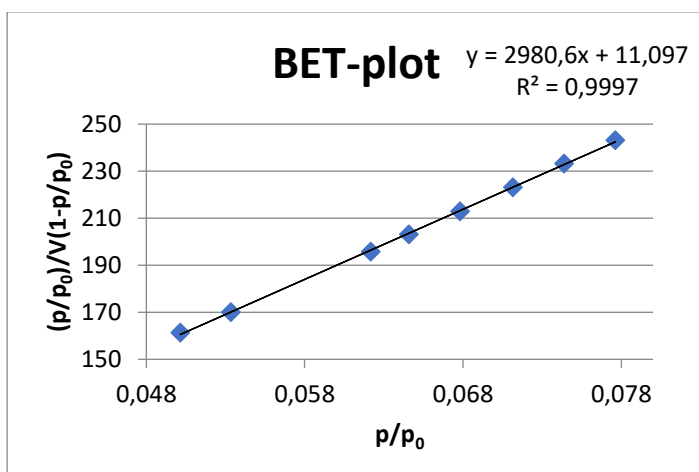*Figure 4-5. N2-sorption of unwashed MOF-808.*

Figure 4-6. BET-plot of unwashed MOF-808.

Figure 4-7 indicates that the surface area after washing increased to 1603 m^2/g, meaning MOF-808 did not have the same surface area as reported, even after washing. Therefore, a better washing procedure is required to obtain the same surface area.
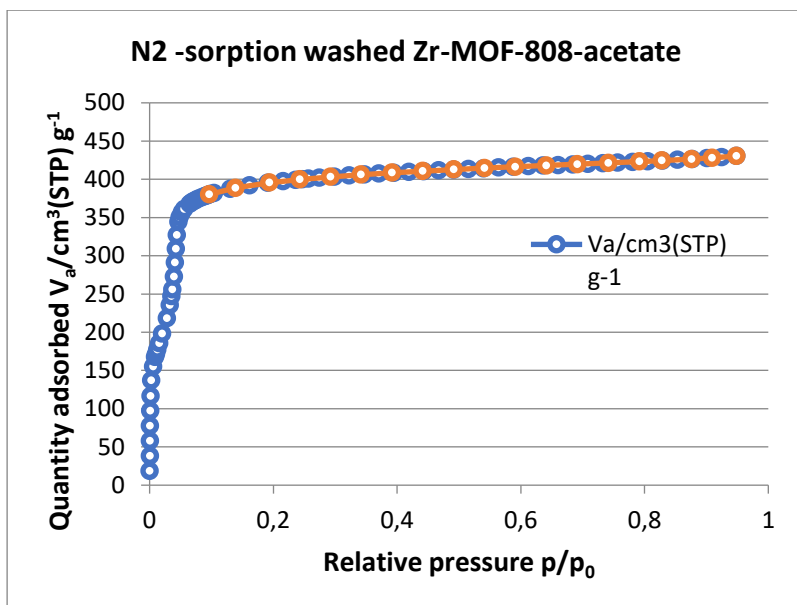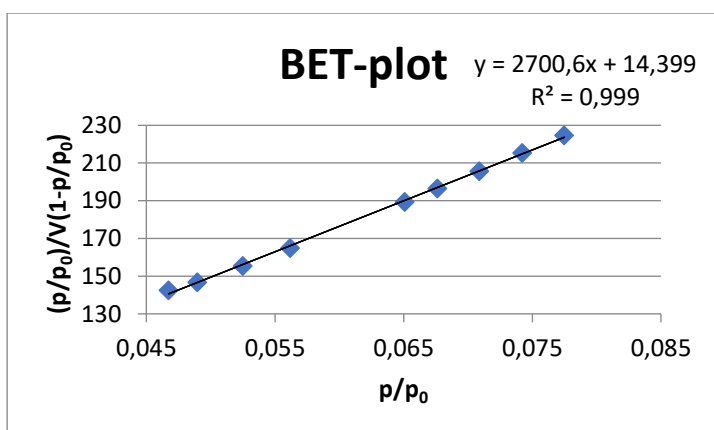
Figure 4-7.

Figure 4-8. BET-plot of surface area.

The calculated BET values are summarized in Table 4-2. The BET surface area was calculated with eq. 7 and total pore volume by eq. 8. Correlation coefficient describes the correlation for the linear points in the BET – plot. For the washed sample the coefficient is 0.9990 and for the unwashed its 0.9997, implying that the fits the plotting. Comparing results for washed and unwashed all values has increased after washing.

Table 4-2. Summarization of the calculated BET-values.

Sample	Surface area (m²/g)	Total pore volume (cm³/g) At 0.9 P/P⁰	Vₘ (cm³(STP)/g)	Corr. coefficient
Unwashed	1455	0.620	334	0.9997
Washed	1603	0.664	368	0.9990

Figure 12 shows XRD that was performed after N_2-adsorption to ensure the structure was still intact and that the structure was stable enough for adsorption. The peaks are still located at the same 2 theta degree, indicating that the structure is still intact after adsorption.
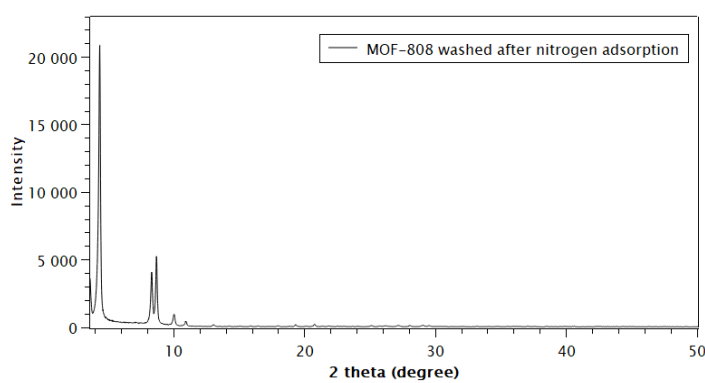
Figure 4-9. XRD plot of MOF-808 after adsorption experiment.

4.5 NMR-analysis:

The molar ratios of molecular species in Zr-MOF-808-Ac were calculated from NMR-plot Equation used to find the ratio of acetic acid to linker:

$$\left(\frac{Acetic\ acid}{Trimesic\ acid}m_R\right) = \frac{\frac{Acetic\ acid\ H^1\ int.}{N_H\ Acetid\ acid}}{\frac{Trimesic\ acid\ int}{N_H\ Trimesic\ Acid}} = \left(\frac{Acetic\ acid\ H^1\ int.}{N_H\ Acetid\ acid}\right) * \frac{N_{HTA}}{TA\ H^1\ Int}$$

Calculations for unwashed MOF-808:

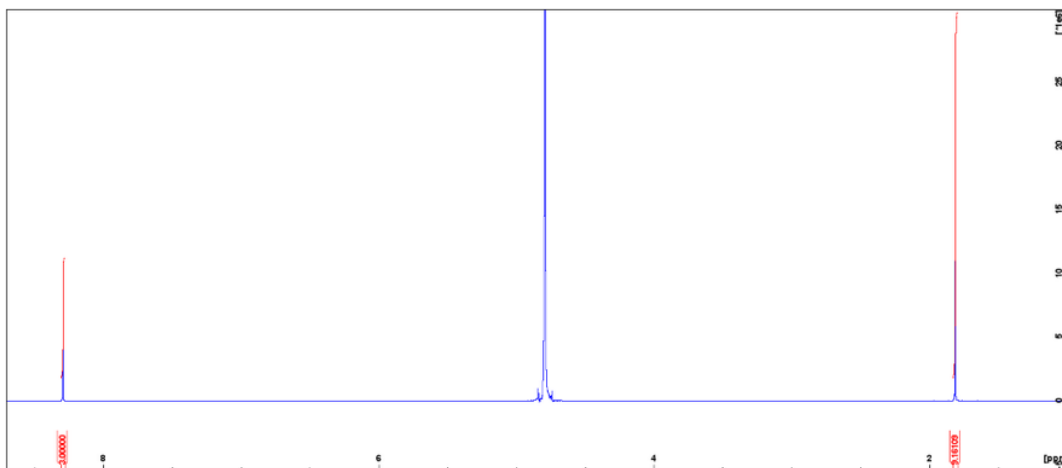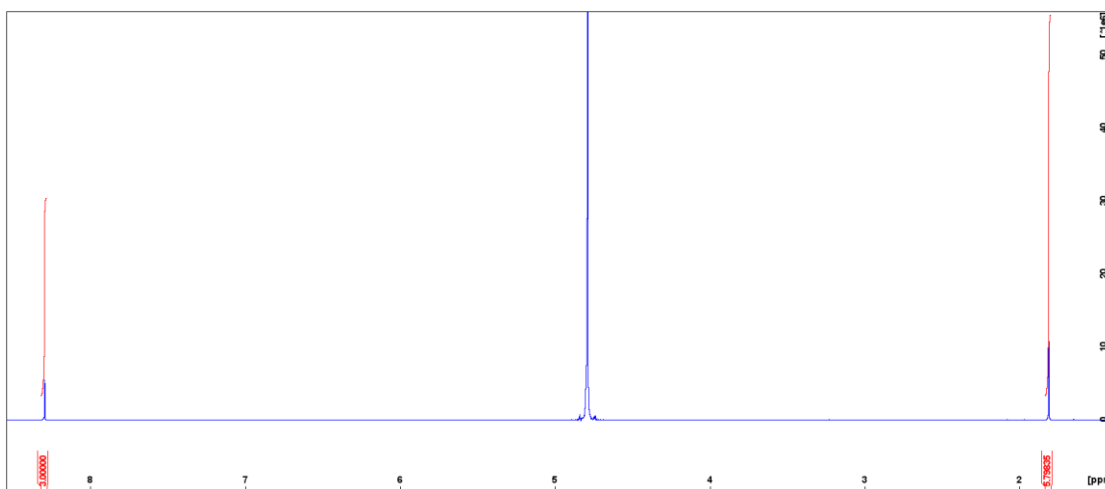$$\frac{Acetic\ acid}{Trimesic\ acid}m_R = \left(\frac{9.17}{3}\right) * \frac{3}{3} = \frac{3.05}{1} = 3.05$$

Figure 4-10. NMR-plot of unwashed Zr-MOF-808-Ac.

Washed MOF-808:

$$\frac{Acetic\ acid}{Trimesic\ acid}\,m_R = \left(\frac{5.79}{3}\right)*\frac{3}{3} = \frac{3.05}{1} = 1.93$$

The ratio for acetic acid and trimesic acid is lower after the washing (1.93) than before (3.05), indicating that the washing has removed some modulator (acetic acid).

Figur 4-11. NMR plot of washed Zr-MOF-808-Ac.

In figure 25 the plot of MOF-808 is compared with plot of acetic acid and trimeric acid. The peaks of trimetric acid and acetic acid in MOF-808 are matching with the single plots of them alone, indicating that there are no impurities in the sample.
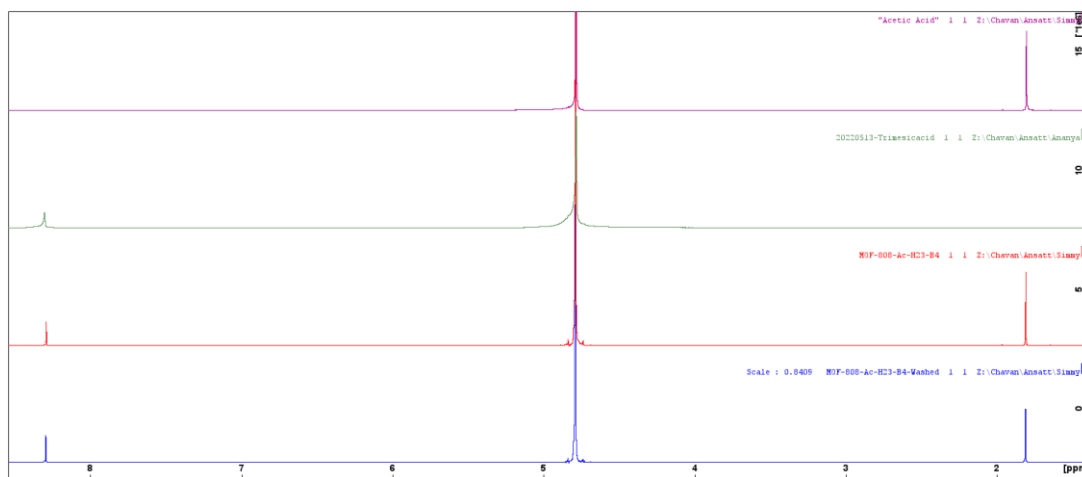
Figure 4-12. NMR plot of washed and unwashed MOF-808 compared to plot with trimesic acid and acetic acid alone.

4.6 SEM-EDS-analysis:

Figure 4-13 illustrates MOF-808-acetate before washing. This was done to examine the morphology of the product and understand the composition/content of the product. The figure indicates that the product has an octahedral morphology.
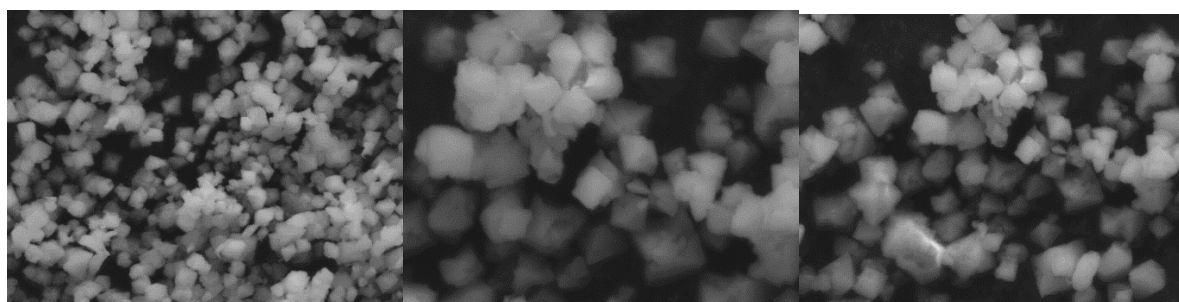

Figure 4-13. Pictures of unwashed MOF-808 taken with the SEM-instrument.

SEM pictures of MOF-808-Acetate after washing with water and acetone, see figure 4-14. The octahedra morphology is still very clear, meaning that the structure is still stable after washing.
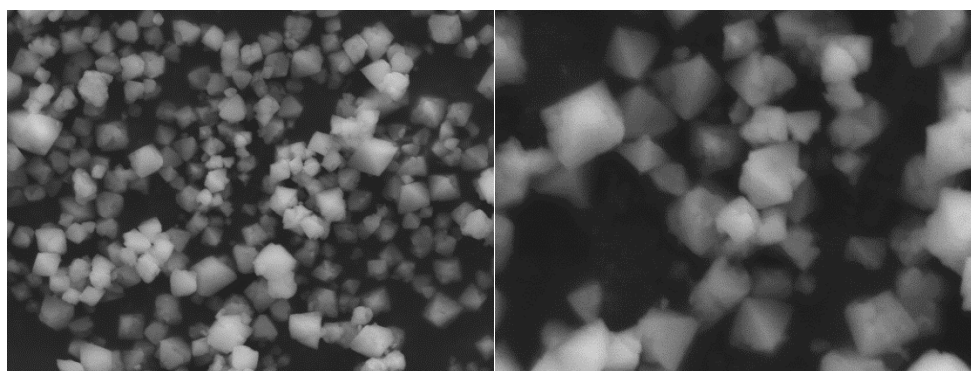

Figure 4-14. SEM picture of Zr-MOF-808 after washing with water and acetone.

EDS was used to find the composition of elements in the samples. The EDS-spectrum of MOF-808 in figure 4-15 indicates a high amount of chlorine (5.12%) although there is no chlorine in MOF-808. This indicates that chlorine, probably from

The high amount of Zr in the samples confirms that Zr-MOF was made. The analysis indicates that there is a significant amount of Cl (5.12%) in the sample. Since there is no chlorine in MOF-808 this indicates that the washing after the synthesis is not successful.
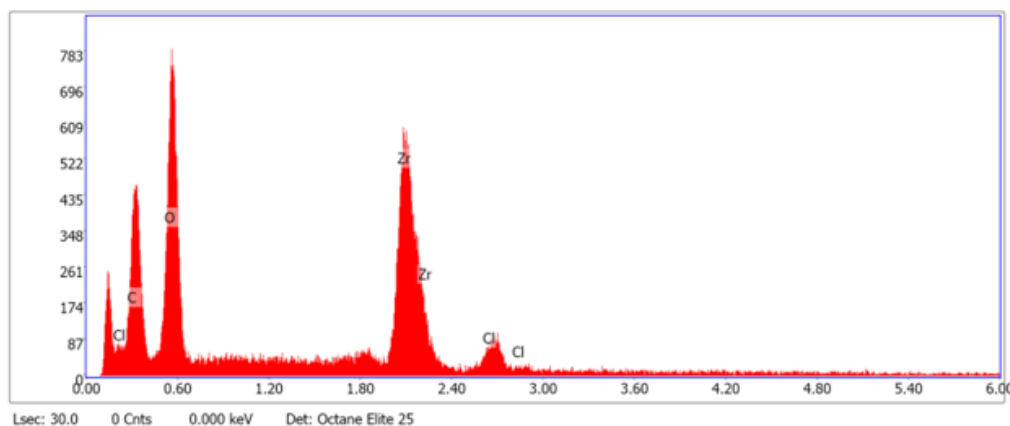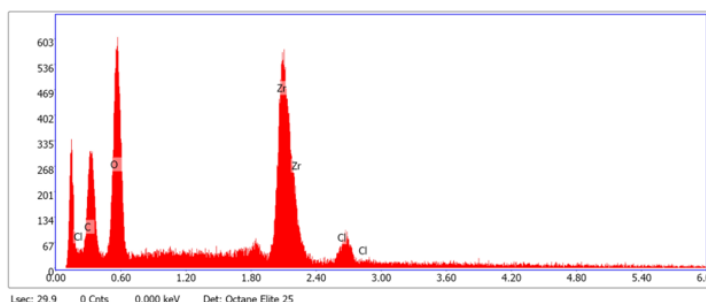

eZAF Smart Quant Results

Element	Weight %	Atomic %	Net Int.	Error %	Kratio	Z	A	F
C K	30.98	49.89	209.78	10.52	0.1106	1.1640	0.3066	1.0000
O K	34.35	41.51	424.81	9.46	0.1403	1.1035	0.3702	1.0000
ZrL	30.92	6.56	256.99	4.01	0.2325	0.7198	1.0437	1.0005
ClK	3.75	2.04	41.81	16.80	0.0311	0.9120	0.9076	1.0020

Figure 4-15. EDS analysis of selected area 2, det 1 of unwashed MOF-808.

Figure 4-16 shows the EDS analysis for the washed sample. The results shows that the samples still contain approximately the same amounts of Zr and Cl, indicating that the washing did not work as expected and more cleaning is required.

eZAF Smart Quant Results

Element	Weight %	Atomic %	Net Int.	Error %	Kratio	Z	A	F
C K	25.47	43.62	120.11	11.86	0.0846	1.1845	0.2804	1.0000
O K	35.91	46.18	340.46	9.54	0.1500	1.1235	0.3718	1.0000
ZrL	34.41	7.76	217.91	4.07	0.2628	0.7337	1.0401	1.0006
ClK	4.20	2.44	35.41	19.35	0.0351	0.9298	0.8959	1.0018

Figure 4-16. EDS analysis of spot 3. det1 of washed MOF-808.

4.7 LC-MS:

A quantitative analysis method for 3 target PFAS, Perfluorooctanoic acid (PFOA), Perfluorobutanesulfonic acid (PFBS) and heptafluorobutyric acid (PFBA) was developed using Acquity Ultra Performance LC (Quattro Premier XE) instrument coupled with MS.

4.7.1 Calibration curves

The calibration curves were extrapolated because the calibration curve originally made with a higher concentration was not linear. This is expected to be because half of the samples was made days before analyzing and the PFAS may have adsorbed to the walls of the sample holders. PFAS calibration curve ranged from 0,0003 mg/L to 0.20 mg/L, using internal calibration for each PFAS.

Figure 4-17 shows the result for one of the points in the PFOA calibration curve. The blue peak is the integrated area and is linear to the concentration. See the appendix for the rest of the results (peaks).
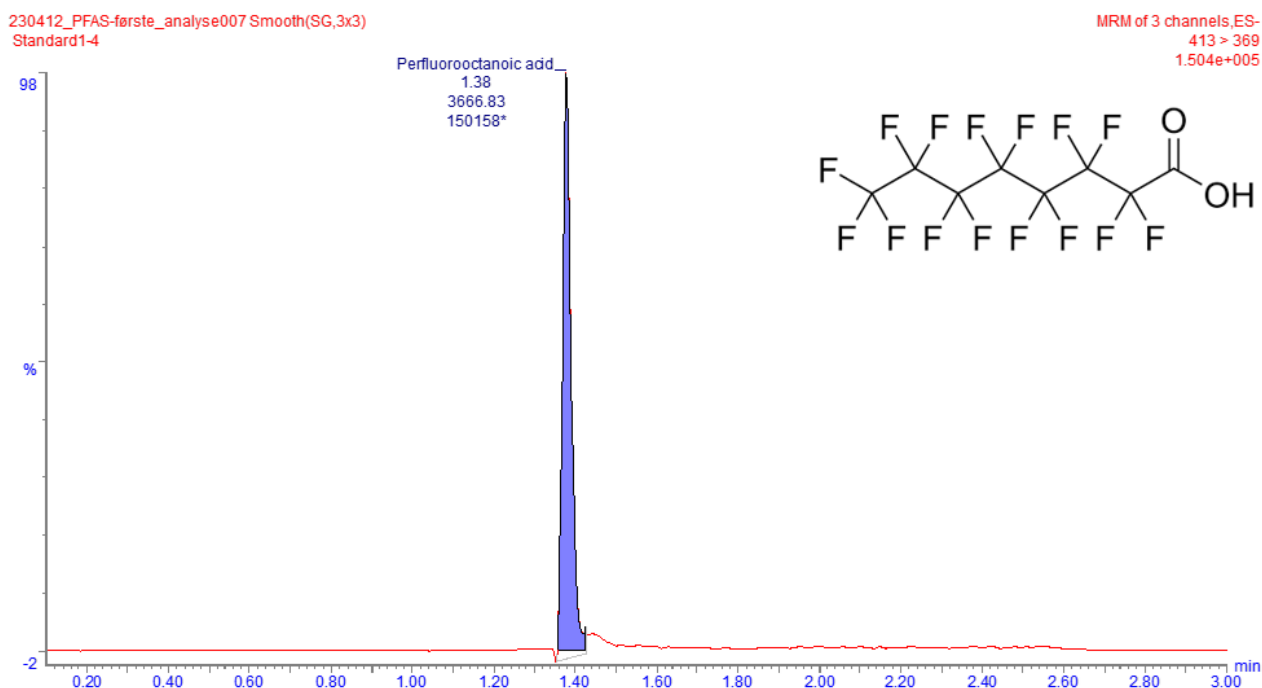
Figure 4-17.

Figure 4-18, 4-19 and 4-20 illustrates the calibration curves for PFOA, PFBS and PFBA. The graphs were extrapolated to find concentrations after adsorption.
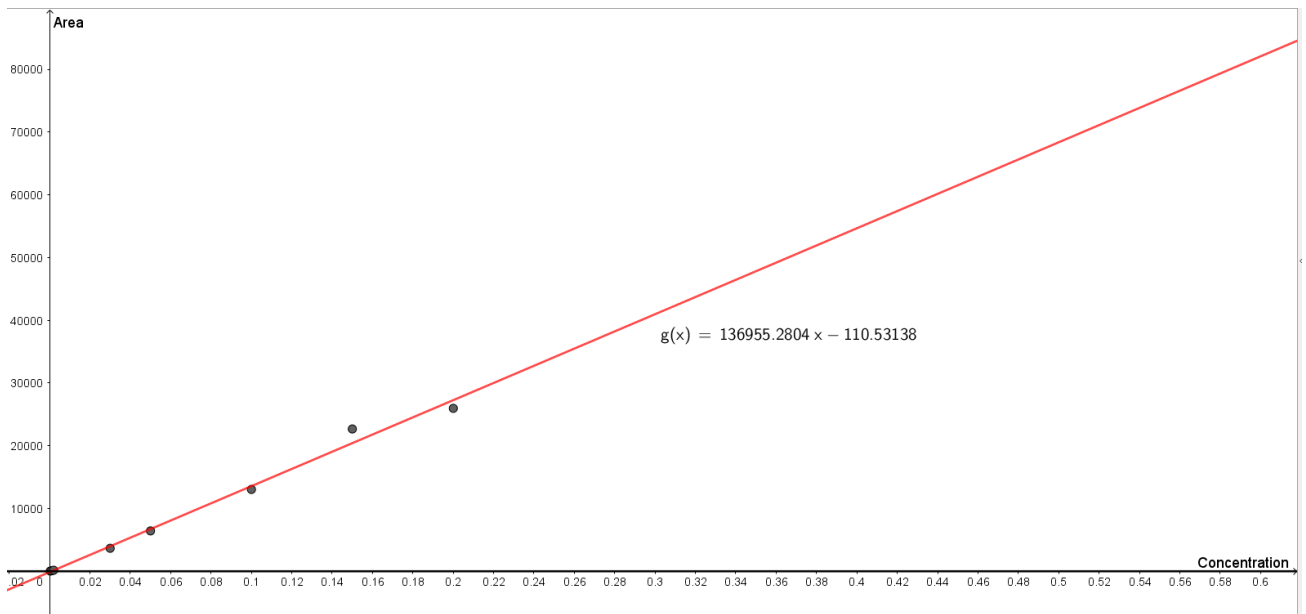
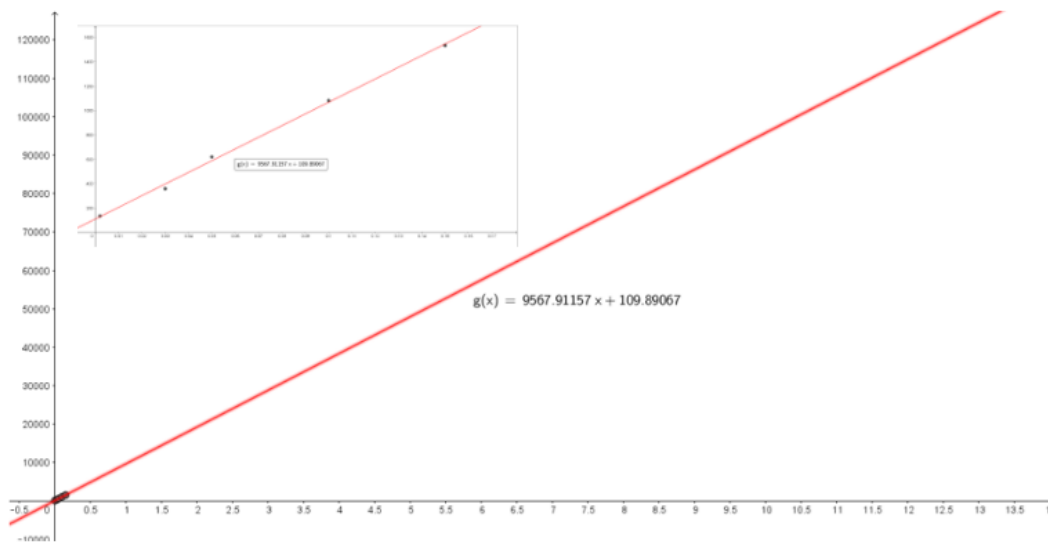*Figure 4-18. Calibration curve for PFOA. $R^2=0.9905$*

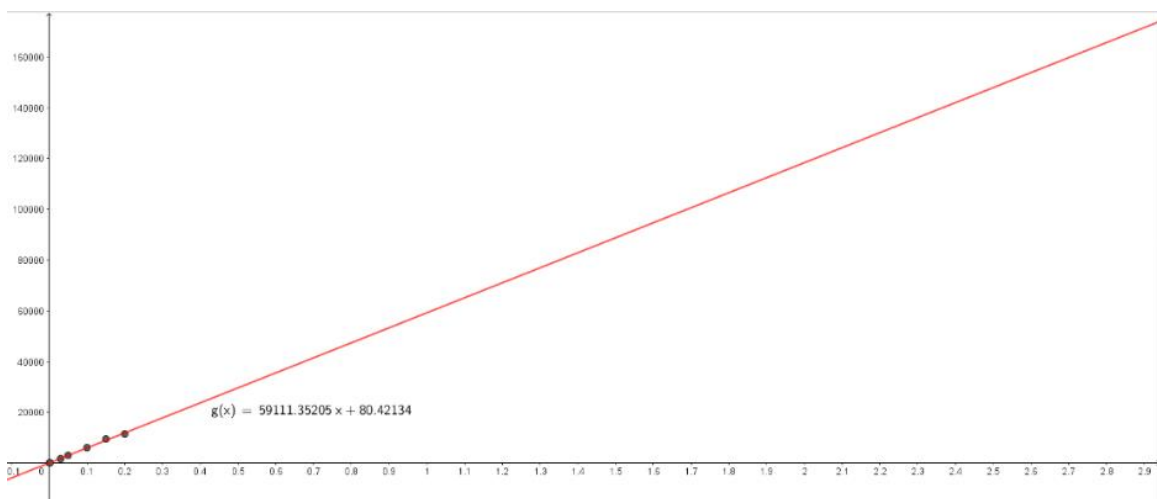*Figure 4-19. Calibration curve for PFBS. $R^2=0.9978$.*

Figure 4-20.

4.7.2 Adsorption experiments

There were performed two adsorption experiments. Experiment 1 was done with initial concentrations of 10 mg/L for each of the PFAS, see table 4-21. The calibration curves for each PFAS were used to find the concentration after adsorption, see the appendix for curves with points. PFOA was 95% adsorbed, PFBS 35% adsorbed and PFBA 74% adsorbed. Indicating that Almost all PFOA was adsorbed, a high uptake of PFBA and a lover adsorption efficiency for PFBS.
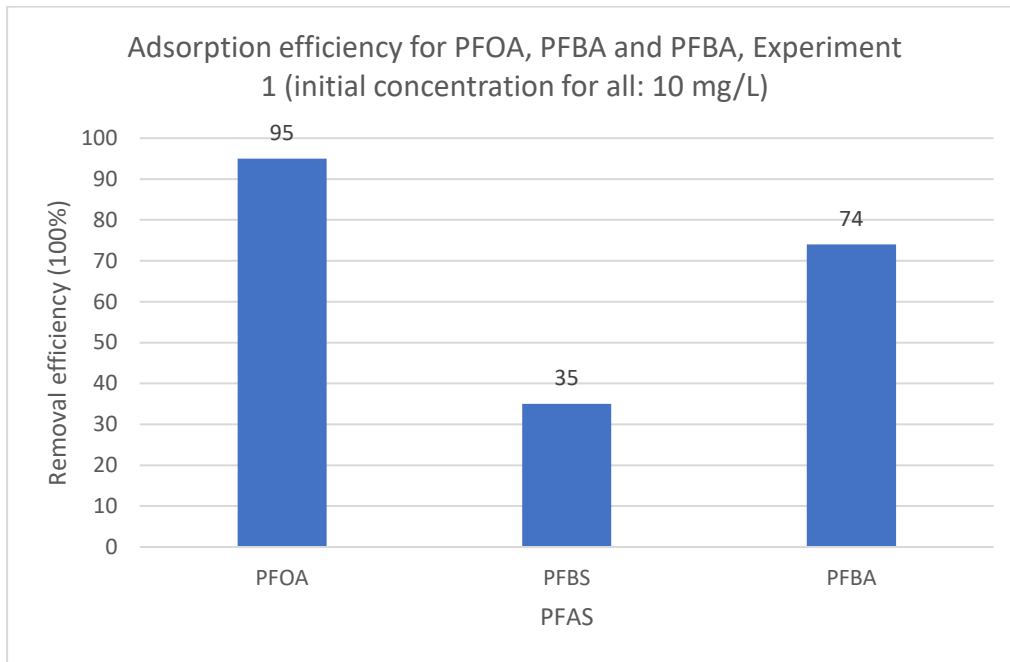

Figure 4-21. Adsorption efficiency for PFOA, PFBA and PFBA in experiment 1. Initial concentrations were 10 mg/L for all.

Experiment 2 was performed with six different concentrations for each PFAS. The removal efficiency was calculated from the concentration before and after adsorption. Figure 4-22 shows the efficiency for PFOA. Sample 1-5 in experiment 2 had so low concentrations that they were set to zero, therefore the efficiency is set to 100%. The

efficiency fits with what is reported on MOF-808 and PFAS, where it often is reported with high efficiency (Chang et al., 2022). See appendix table x with initial concentrations, concentrations after adsorption and area of peaks.
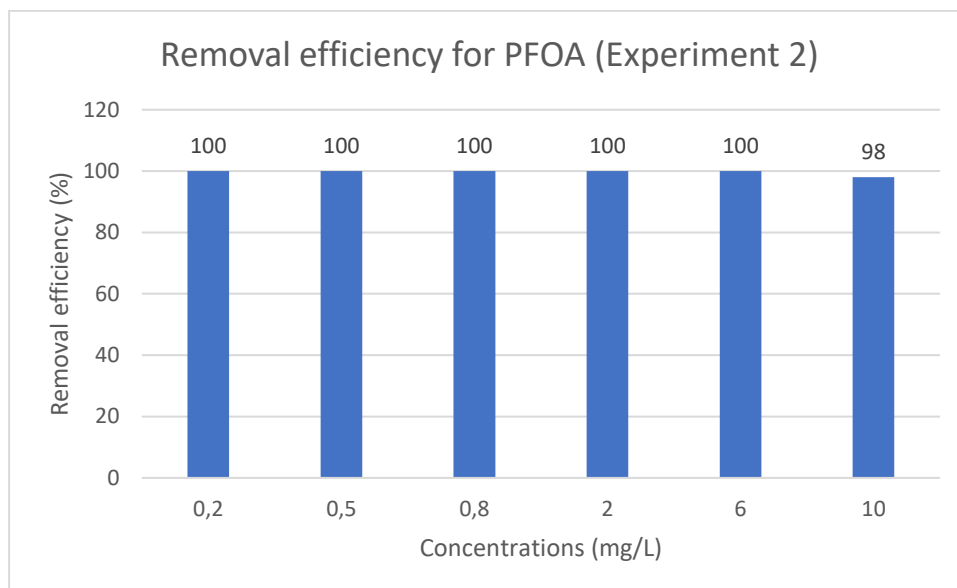

Figure 4.22. Adsorption efficiency for PFOA with 0.2, 0.5, 0.8, 2, 6 and 10 mg/L.

The removal efficiency for PFBS indicated a low uptake on MOF-808, see figure 4-23. The sample with an initial concentration of 0.2 mg/L points out with a 100% efficiency indicating that there may be human errors in the analysis or that PFBS may adsorb better at lower concentrations. The rest of the samples have a negative adsorption efficiency, meaning that the concentration after adsorption is higher than the initial concentration. The low adsorption uptake could be because the sulfuric acid part adsorbs poorly to MOF-808, but there is no reported literature supporting that. The reason for the higher concentrations after adsorption for many of the samples may be contaminated due to the use of the same syringes when filtrating before analysis. Another error source could be that there were no blanks samples between each sample to avoid contamination (Øiestad, 2018).
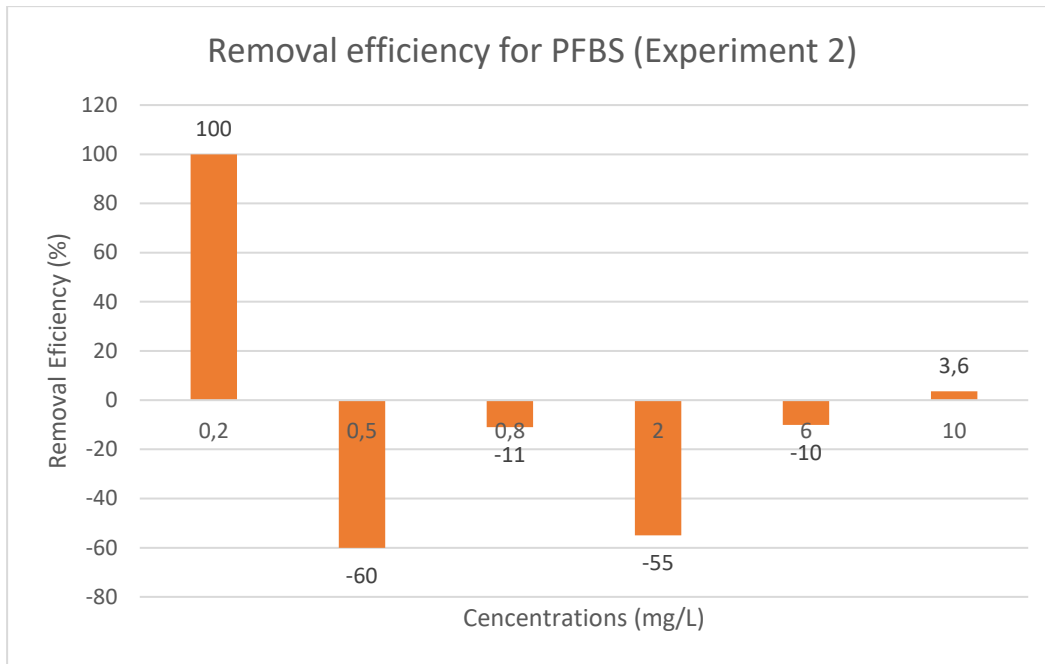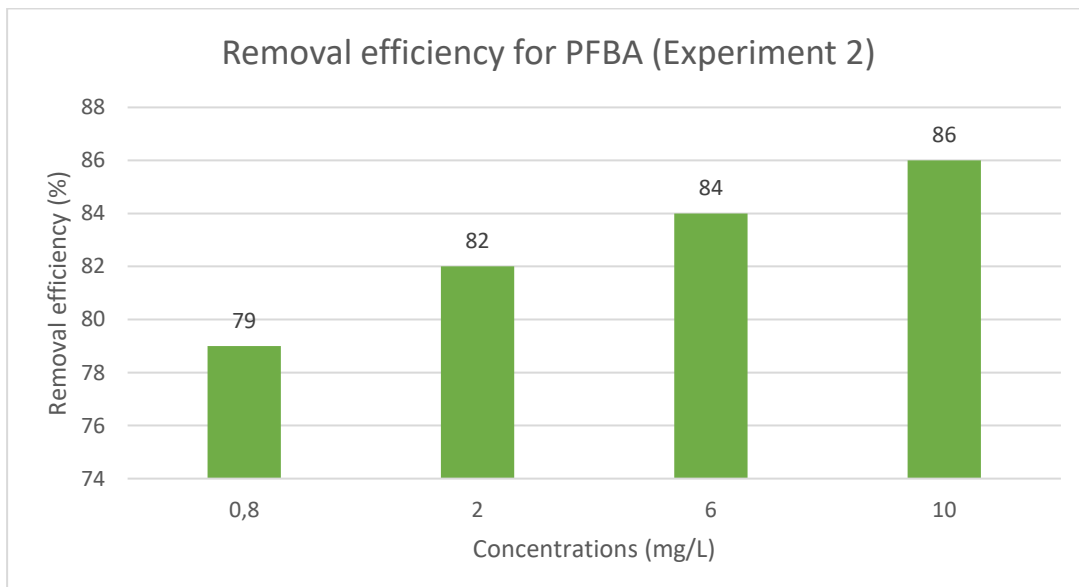
Figure 4-23. Adsorption efficiency for PFBS with 0.2, 0.5, 0.8, 2, 6 and 10 mg/L.

The efficiency removal for PFBA, see table 4-24, shows an increasing removal efficiency with increasing initial concentrations. The removal efficiency is between 79 to 86 % percent which is a high uptake but would have been better with even higher. These results are a bit lower than reported in literature. Would be interesting to examine the uptake with a wider range of concentrations.

*Figur 4-24. Adsorption efficiency for PFBA with 0.8, 2, 6 and 10 mg/L.*

PFAS are highly stable components, and this makes them hard to work with in experiments. They can contaminate easily from sample to sample or from equipment that is not washed

properly, this may increase the concentration. To avoid contamination PFAS-free materials should have been used, high-grade solvents on the equipment used. Since the blank samples contained some PFAS, see figure x, it is important to take into account that the water may have some PFAS in it, and this may influence the results. When solutions are stored in vials over time the components may adsorb on to the glass and ensure that the concentrations decrease before analysis. The solution may not be homogeneous after storing for a while; therefore, a vortex should be used for the vials with samples before analyzing. This was not performed in this project and could have given more accurate results. The vials with samples were made and stored at different times in this project. The optimal procedure is to make the samples at the same time and not store them long before analysis, to prevent the vials from adsorbing any compounds. Another precaution is to have a blank sample between each sample in the instrument, or at least have a blank sample between each type of PFAS. Interesting to see if experiments with these modifications could have given different results (Øiestad, 2018).
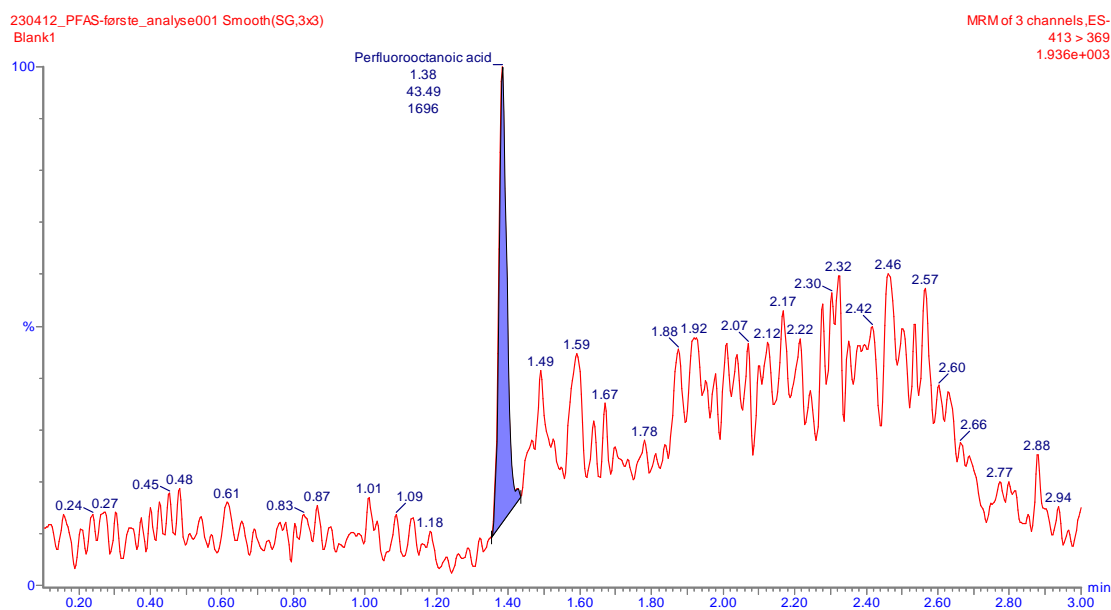

Figur 4-25. Peak results after analyzing a sample that were supposed to be distilled water. This could mean that the water in the sinks at UiS contains a small amount of PFAS, or that the samples were contaminated under the preparation.

XRD was performed after adsorption experiment 1 to examine the crystallinity after adsorption, see figure 4-26. The peaks are located at the same points, indicating that the structure is still intact after adsorption. The intensity changed a bit in some of the samples, this could be because of the change in structure after adsorbing PFAS (Chang et al., 2022).
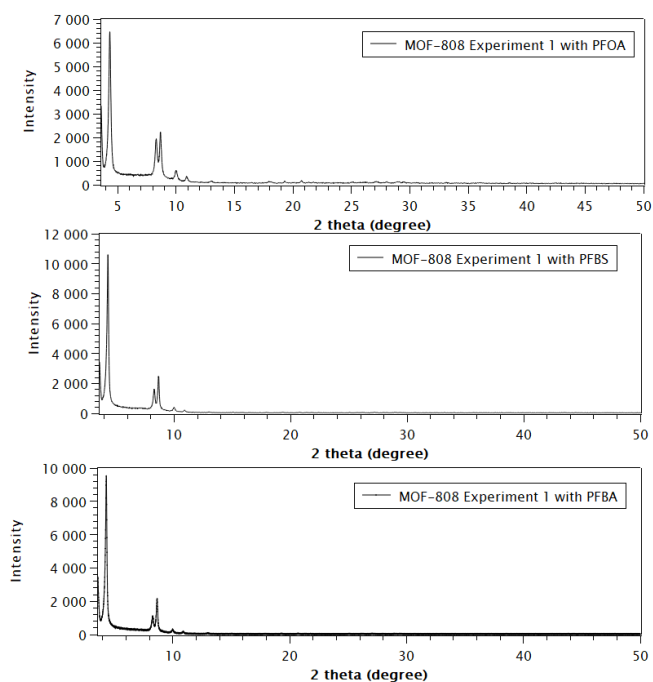
Figur 4-26. XRD plots for MOF-808 after adsorption of PFOA, PFBS and PFBA.

XRD was performed after experiment 2 where three different PFAS was adsorbed on MOF-808, see figure 4-27. The diffraction points are still in the same place, implying that the structure is still undamaged/complete/intact. Also here it is with a bit of difference in intensity suggesting a change in the structure because of the adsorbed PFAS (Chang et al., 2022).
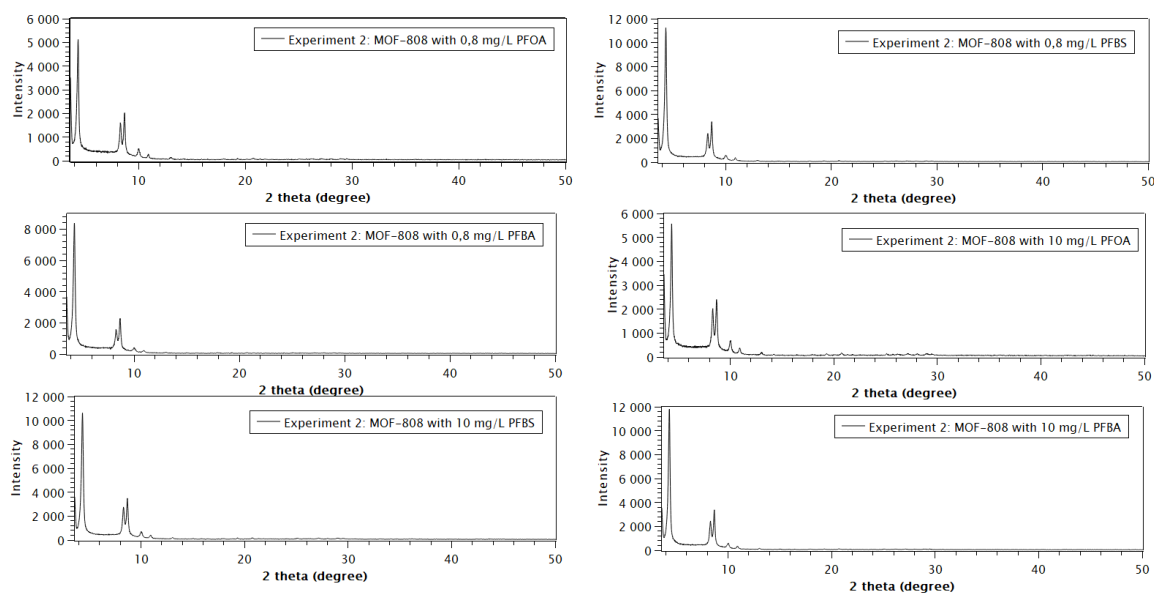
Figur 4-27. Figure 4-27: XRD plot of MOF-808 after adsorption experiments.

5. Conclusion:

XRD, TGA, SEM-EDS, NMR and N_2-sorption indicated a successful synthesis of MOF-808 with the structure and composition. Acetone wash raised the surface area from 1455 m^2/g to 1603 m^2/g indicating that with further optimizing of the washing protocol the surface area could reach up to the reported area (1946 m^2/g) (Aunan et al., 2021). EDS analysis indicated a high amount of Cl. This means that the post-synthesis washing was not successful and needs further optimization. Washing over night and repetitively can be the solution to both problems.

A method to quantify the PFAS concentration in water with the LC-MS instrument is successfully developed. Although the method still needs more development regarding sample treatment and preparation to get an optimal protocol.

The adsorption efficiency variated for each PFAS. The uptake of MOF-808 adsorbs on PFOA was nearly 100% on all concentrations. The uptake of PFBS were negative, indicating no adsorbed PFBS and contaminatinon of samples. This could either mean that MOF-808 needs more cleaned pores to adsorb PFBS or that it is unable to adsorb the compound. The uptake of PFBA was high, between 80 and 90%. These results indicates that MOF-808 adorbs PFAS with carboxylic groups good, and the longer chains better than the shorter chains.

In this project I have learned how to synthesize MOFs and have been participating in the development of detection of PFAS, with the use of a LC-MS instrument. I have learned about PFAS and how important it is to find ways to remove pollutants from drinking water. XRD, TGA, SEM-EDS, NMR and N_2-sorption are some instruments I have learned how to use. In addition, I have learned how to find information and read about an area of research that is developing fast.

Further work:

MOF-808: develop a proper washing protocol to get a higher surface area and get rid of the unwanted Cl in the pores. It could help with washing overnight and more times with acetone. The stability of MOF-808 with different pH and temperature should be investigated closer.

PFAS adsorption: A wider range of concentrations should be tested for adsorption, and concentrations closer to what is found in drinking water around the world. Other PFAS should

be tested, with a wider range of longer/shorter chains and with different functional groups. Since MOF-808 may have problems with adsorbing there would be interesting to examine if more washing to empty the pores could improve the uptake or to synthesize another MOF with different pore sizes to investigate if there is any difference. NU-1000 is another Zirconium-based MOF that has been reported to have a high adsorption efficiency of PFBS. Or a regeneration of the adsorbent should be investigated? (Li et al., 2021).

LC-MS instrument: Optimize protocol for preparing the samples for both calibration curves and for samples used in adsorption experiments. This could give more accurate results, implying a more linear calibration curve. The protocol should include a maximum storing time before analysis and how to clean equipment before use. Further, it would be interesting to investigate the limit of detection (log) and limit of quantification (lod) for the LC-MS instrument.

6. References:

Adsorption Isotherm and Its Types—Chemistry Notes. (u.å.). Hentet 15. mai 2023, fra

https://chemistnotes.com/physical/adsorption-isotherm-and-its-types/

All news—ECHA. (u.å.). Hentet 13. mai 2023, fra https://echa.europa.eu/-/echa-publishes-

pfas-restriction-proposal

Altarawneh, M. (2021). A closer look into the contribution of atmospheric gas-phase

pathways in the formation of perfluorocarboxylic acids. *Atmospheric Pollution

Research*, *12*(12), 101255. https://doi.org/10.1016/j.apr.2021.101255

Andreassen, R. N. (2023, januar 3). *Dyr og fugler får i seg flere miljøgifter enn forventet*.

NRK. https://www.nrk.no/tromsogfinnmark/dyr-og-fugler-far-i-seg-flere-miljogifter-

enn-forventet-1.16238046

Aunan, E., Affolter, C. W., Olsbye, U., & Lillerud, K. P. (2021). Modulation of the

Thermochemical Stability and Adsorptive Properties of MOF-808 by the Selection of

Non-structural Ligands. *Chemistry of Materials*, *33*(4), 1471–1476.

https://doi.org/10.1021/acs.chemmater.0c04823

bell. (2019, juli 22). Per- and Polyfluoroalkyl Substances (PFAS). *PPM Consultants*.

https://www.ppmco.com/per-and-polyfluoroalkyl-substances-pfas/

Brendel, S., Fetter, É., Staude, C., Vierke, L., & Biegel-Engler, A. (2018). Short-chain

perfluoroalkyl acids: Environmental concerns and a regulatory strategy under

REACH. *Environmental Sciences Europe*, *30*(1), 9. https://doi.org/10.1186/s12302-

018-0134-4

Canada, H. (2017, mars 12). *Long-chain Perfluorocarboxylic Acids (PFCAs), their salts, and

their precursors—Information sheet* [Frequently asked questions].

https://www.canada.ca/en/health-canada/services/chemical-substances/fact-

sheets/chemicals-glance/long-chain-perfluorocarboxylic-acids-pfcas-salts-precursors.html

Chang, P.-H., Chen, C.-Y., Mukhopadhyay, R., Chen, W., Tzou, Y.-M., & Sarkar, B. (2022). Novel MOF-808 metal–organic framework as highly efficient adsorbent of perfluorooctane sulfonate in water. *Journal of Colloid and Interface Science*, *623*, 627–636. https://doi.org/10.1016/j.jcis.2022.05.050

Chemical structure of perfluorooctanoic acid (PFOA). (u.å.). ResearchGate. Hentet 31. januar 2023, fra https://www.researchgate.net/figure/Chemical-structure-of-perfluorooctanoic-acid-PFOA_fig1_328674109

Chemyx. (2017, november 8). *Basic Principles of HPLC, MS & LC-MS*. Chemyx Inc. https://chemyx.com/support/knowledge-base/application-reference-by-topic/basic-principles-hplc-ms-lc-ms/

Cserbik, D., Redondo-Hasselerharm, P. E., Farré, M. J., Sanchís, J., Bartolomé, A., Paraian, A., Herrera, E. M., Caixach, J., Villanueva, C. M., & Flores, C. (2023). Human exposure to per- and polyfluoroalkyl substances and other emerging contaminants in drinking water. *Npj Clean Water*, *6*(1), Artikkel 1. https://doi.org/10.1038/s41545-023-00236-y

Effects of PFAS on human health—European Environment Agency. (u.å.). [Infographic]. Hentet 17. mars 2023, fra https://www.eea.europa.eu/signals/signals-2020/infographics/effects-of-pfas-on-human-health/view

Farha, O. K., Özgür Yazaydın, A., Eryazici, I., Malliakas, C. D., Hauser, B. G., Kanatzidis, M. G., Nguyen, S. T., Snurr, R. Q., & Hupp, J. T. (2010). De novo synthesis of a metal–organic framework material featuring ultrahigh surface area and gas storage capacities. *Nature Chemistry*, *2*(11), Artikkel 11. https://doi.org/10.1038/nchem.834

Fast and High-Resolution LC-MS Separation of PFAS. (u.å.). Hentet 13. mai 2023, fra

   https://www.sigmaaldrich.com/NO/en/technical-documents/technical-

   article/environmental-testing-and-industrial-hygiene/waste-water-and-process-water-

   testing/fast-and-high-resolution-lc-ms-separation-of-pfas

FitzGerald, L. I., Olorunyomi, J. F., Singh, R., & Doherty, C. M. (2022). Towards Solving the

   PFAS Problem: The Potential Role of Metal-Organic Frameworks. *ChemSusChem*,

   15(19), e202201136. https://doi.org/10.1002/cssc.202201136

Forslag om å forby alle PFAS-er lanseres i Brussel—Miljødirektoratet. (u.å.).

   Miljødirektoratet/Norwegian Environment Agency. Hentet 3. februar 2023, fra

   https://www.miljodirektoratet.no/aktuelt/arrangementer/2023/februar-2023/forslag-

   om-a-forby-alle-pfaser-lanseres-i-brussel/

Haug, L. S., Knutsen, H. K., & Thomsen, C. (2018a, desember 13). *Fakta om PFAS*.

   Folkehelseinstituttet. https://www.fhi.no/ml/miljo/miljogifter/fakta/fakta-om-pfos-og-

   pfoa/

Haug, L. S., Knutsen, H. K., & Thomsen, C. (2018b, desember 13). *PFAS og helseeffekter*.

   Folkehelseinstituttet. https://www.fhi.no/ml/miljo/miljogifter/fakta/fakta-om-pfos-og-

   pfoa/

Holder, C. F., & Schaak, R. E. (2019). Tutorial on Powder X-ray Diffraction for

   Characterizing Nanoscale Materials. *ACS Nano*, *13*(7), 7359–7365.

   https://doi.org/10.1021/acsnano.9b05157

jnelson. (2022, mars 16). *Notification Level Recommendation for Perfluorohexane Sulfonic

   Acid (PFHxS) in Drinking Water* [Text]. OEHHA.

   https://oehha.ca.gov/water/report/notification-level-recommendation-perfluorohexane-

   sulfonic-acid-pfhxs-drinking-water

Karbassiyazdi, E., Kasula, M., Modak, S., Pala, J., Kalantari, M., Altaee, A., Esfahani, M. R., & Razmjou, A. (2023). A juxtaposed review on adsorptive removal of PFAS by metal-organic frameworks (MOFs) with carbon-based materials, ion exchange resins, and polymer adsorbents. *Chemosphere*, *311*. Scopus. https://doi.org/10.1016/j.chemosphere.2022.136933

Kolesnik, O. (2020, juli 21). *Perfluorobutyric Acid (PFBA)*. SIELC Technologies. https://sielc.com/perfluorobutyric-acid

Pedersen, B. (2023). Fluor. I *Store norske leksikon*. http://snl.no/fluor

Perfluorbutansulfonsäure. (2021). I *Wikipedia*. https://de.wikipedia.org/w/index.php?title=Perfluorbutansulfons%C3%A4ure&oldid=214429898

Perfluorerte stoffer (PFOS, PFOA og andre PFAS-er). (u.å.). Miljøstatus. Hentet 16. januar 2023, fra https://miljostatus.miljodirektoratet.no/tema/miljogifter/prioriterte-miljogifter/perfluorerte-stoffer-pfos-pfoa-og-andre-pfas-er/

PFAS and Home Treatment of Water—MN Dept. Of Health. (u.å.). Hentet 14. mai 2023, fra https://www.health.state.mn.us/communities/environment/hazardous/topics/pfashometreat.html

PFAS removal by ion exchange resins: A review | Elsevier Enhanced Reader. (u.å.). https://doi.org/10.1016/j.chemosphere.2021.129777

PFOS and Groundwater. (u.å.).

Powder X-ray Diffraction. (2013, oktober 2). Chemistry LibreTexts. https://chem.libretexts.org/Bookshelves/Analytical_Chemistry/Supplemental_Modules_(Analytical_Chemistry)/Instrumentation_and_Analysis/Diffraction_Scattering_Techniques/Powder_X-ray_Diffraction

Renner, R. (2006). The long and the short of perfluorinated replacements. *Environmental Science & Technology*, *40*(1), 12–13. https://doi.org/10.1021/es062612a

SEM/EDS Analysis | RTI Laboratories. (2016, februar 22). https://rtilab.com/techniques/sem-eds-analysis/

Shen, H., Gao, M., Li, Q., Sun, H., Jiang, Y., Liu, L., Wu, J., Yu, X., Jia, T., Xin, Y., Han, S., Wang, Y., & Zhang, X. (2023). Effect of PFOA exposure on diminished ovarian reserve and its metabolism. *Reproductive Biology and Endocrinology*, *21*(1), 16. https://doi.org/10.1186/s12958-023-01056-y

Thommes, M., Kaneko, K., Neimark, A. V., Olivier, J. P., Rodriguez-Reinoso, F., Rouquerol, J., & Sing, K. S. W. (2015). Physisorption of gases, with special reference to the evaluation of surface area and pore size distribution (IUPAC Technical Report). *Pure and Applied Chemistry*, *87*(9–10), 1051–1069. https://doi.org/10.1515/pac-2014-1117

US EPA CENTER FOR PUBLIC HEALTH & ENVIRONMENTAL ASSESSMENT, C. & P. A. D., & Kraft, A. (u.å.). *IRIS Toxicological Review of Perfluorohexanoic Acid (PFHxA) and Related Salts (Public Comment and External Review Draft)* [Reports & Assessments]. Hentet 3. mars 2023, fra https://cfpub.epa.gov/ncea/iris_drafts/recordisplay.cfm?deid=352767

Vann, N. (Regissør). (2022, mars 17). *268_PFAS_med_sofaprat*. https://vimeo.com/689317868/12bcb40e40

Wei, F., Chen, D., Liang, Z., Zhao, S., & Luo, Y. (2017). Synthesis and characterization of metal–organic frameworks fabricated by microwave-assisted ball milling for adsorptive removal of Congo red from aqueous solutions. *RSC Advances*, *7*(73), 46520–46528. https://doi.org/10.1039/C7RA09243A

Appendix 1: Procedures

Procedure for LC-MS computer before analysis:

Masslynx, inlet method, standalone console and MS tune were opened on the computer. In the MS tune window "PFAS Hanna" was opened as a file, then the button "AP I gas" was pressed. Next the "COL gas" button was pressed in the same window. Further the MS tune window was opened and the "Press for operate (stanby) was pressed. The button then went from red to green, signalizing successful protocol so far. Then Standalone console was opened and these buttons were pressed in order: "system", "control" and "start up". Then the "Start" button was pressed and waited 5 to 6 minutes. Inlet window was opened, and the following buttons were pressed: "File", "open", "PFASHANNAA2B1", "open", "LC", "Load method", and it was waited 10 minutes for the gas to be stabile around 400 for 10 minutes. Then mass lynx was opened and the file "PFASHANNA" was opened. The sample specifications were filled in. Then all samples that were to be analyzed were marked and the "Play" button were pressed followed by "OK". The procedure was successful if the first sample turned green in the file.

To look at the results all the wanted samples were marked and "Target lynx" followed by "Process samples" were pressed. It was checked that the right method and samples were analyzed and then "OK" was pressed.

Appendix 2

Figures of integrated area after LC-MS analysis:

The integrated area of each sample containing the three different PFAS. Be aware that the area on the pictures may be different from the numbers used to find the unknown concentrations in the thesis. This is because the figure in the Appendix is not edited like the numbers used in the results.
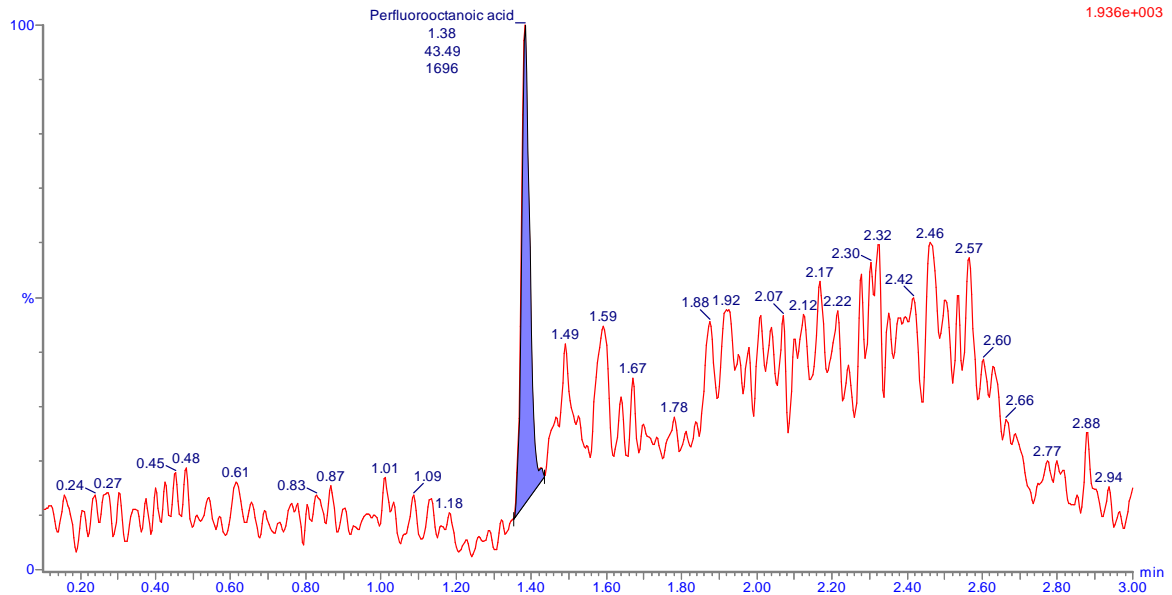
Figure A-1. Blank sample, a small amount of PFOA detected.
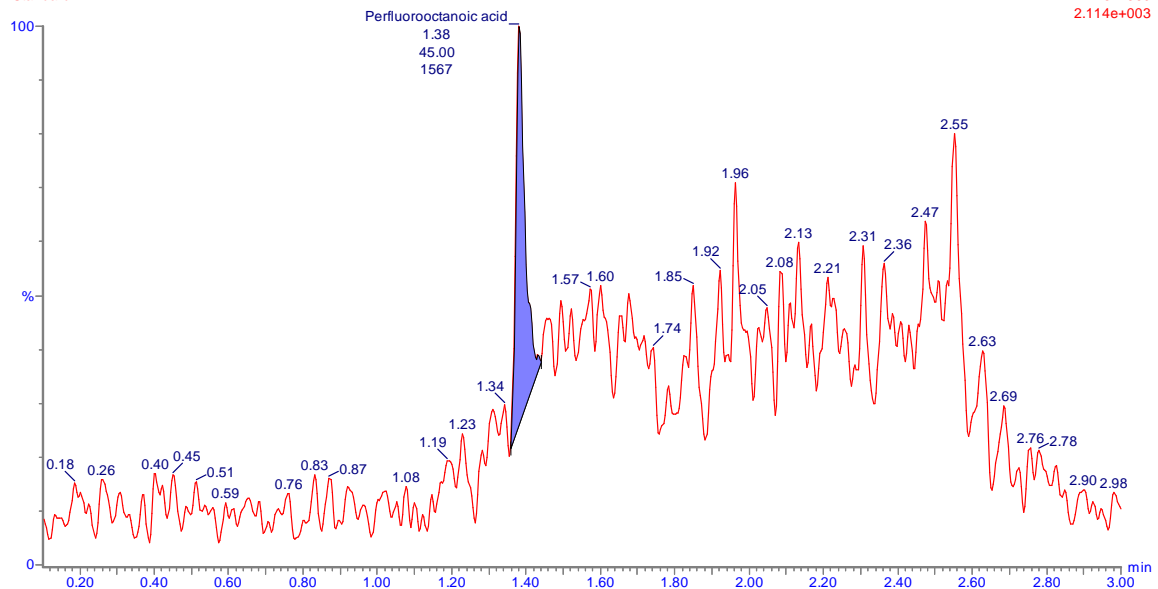
Figur A-2. PFOA detected, 0.0003 mg/L.

Perfluorooctanoic acid
1.38
34.04
1231
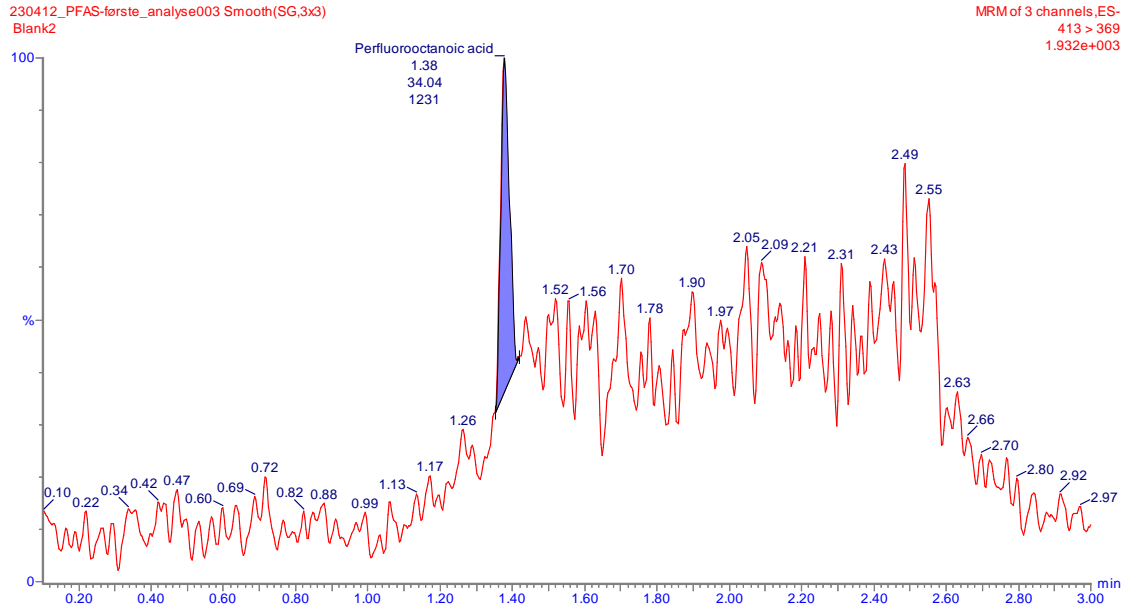
Figure A-3. Blank sample, PFOA detected.

Perfluorooctanoic acid
1.38
171.58
7184
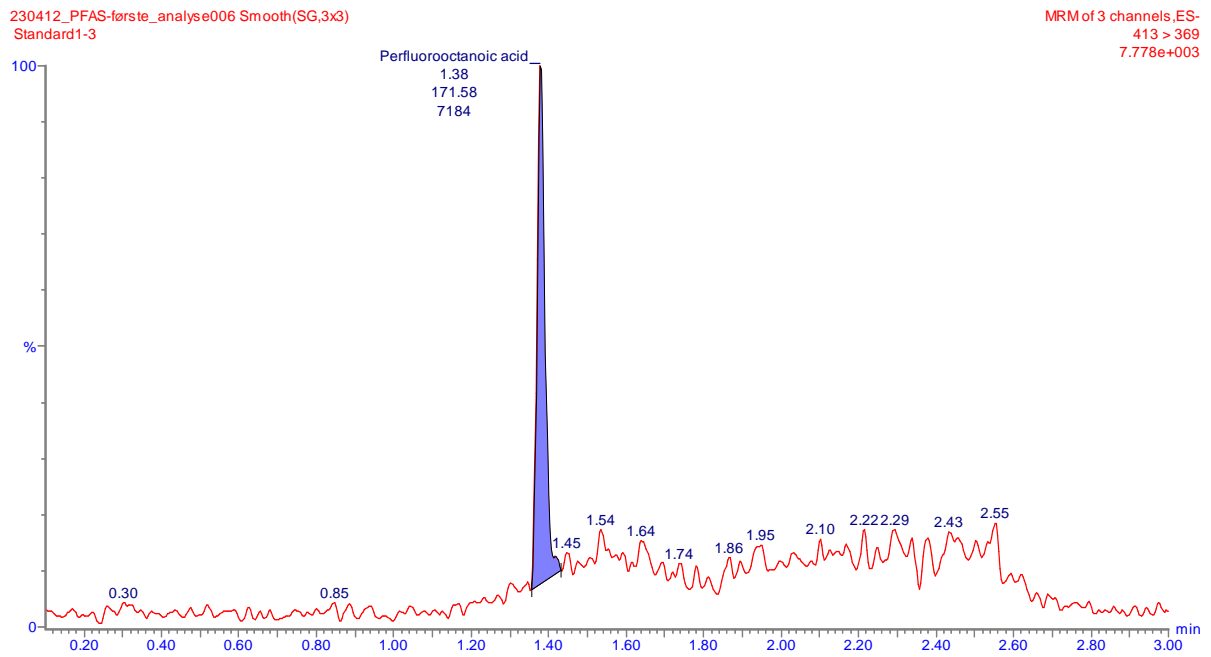
Figure A-4. PFOA detected, 0.002 gm/L.

Perfluorooctanoic acid
1.38
98.67
4318
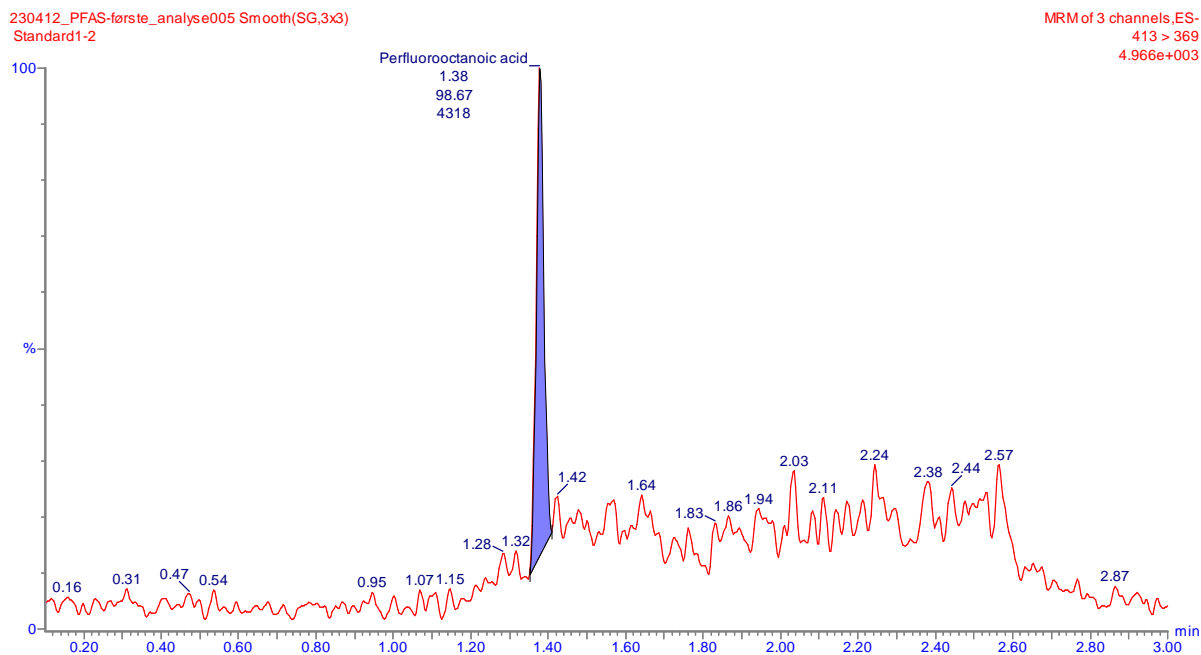
Figure A-5. PFOA detected, 0.001 gm/L.

Perfluorobutanesulfonic acid
1.30
16.38
691
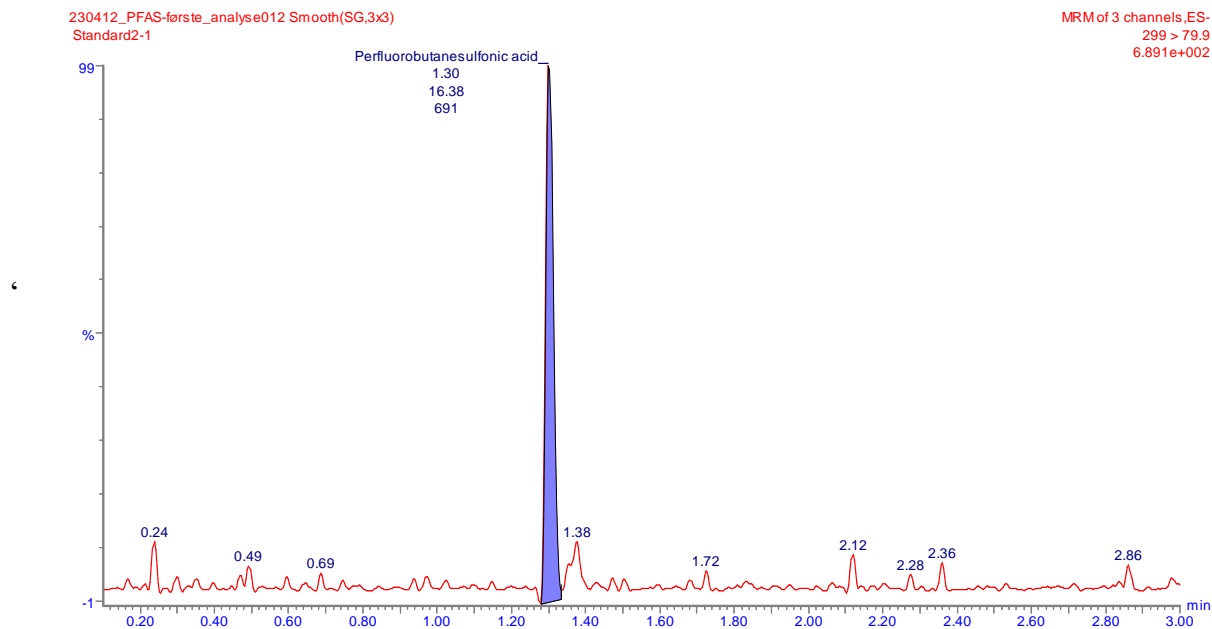
Figure A-6. PFBS detected, 0.0003 gm/L.

51

Perfluorooctanoic acid_
1.38
6336.04
251885*

Figure A-7. PFOA detetcted, 0.05 gm/L.

Perfluorooctanoic acid_
1.38
41.06
1414
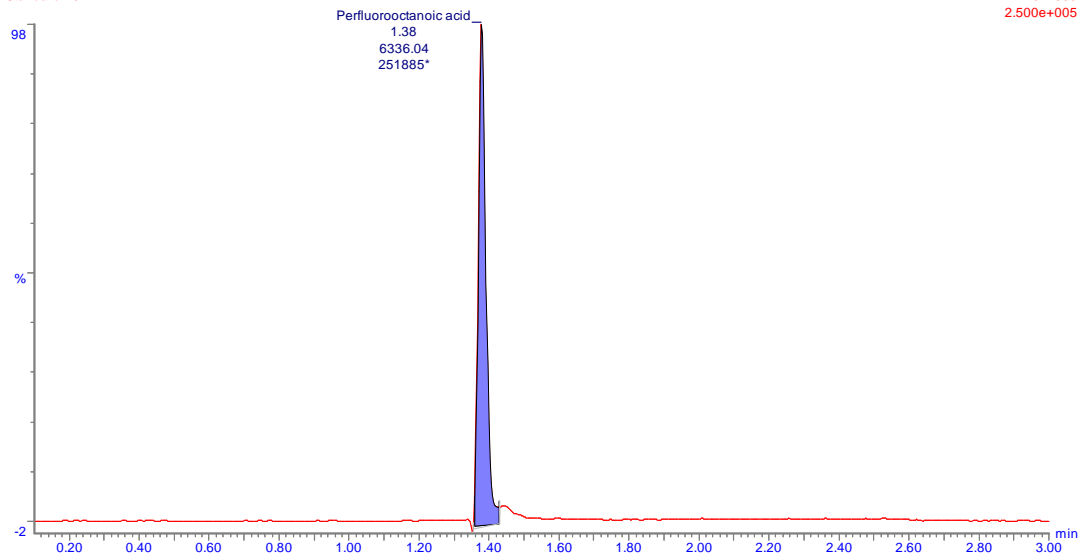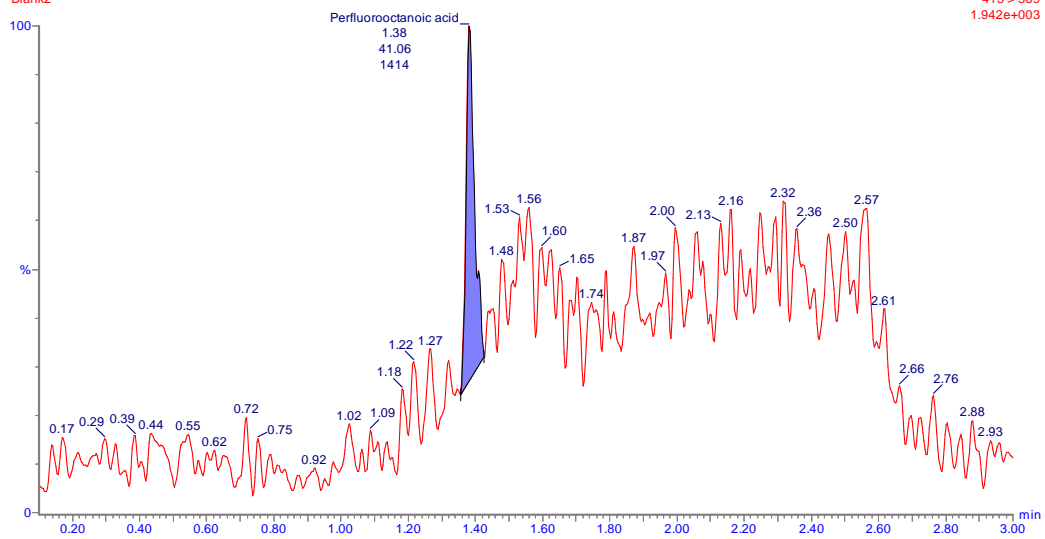
Figure A-8. Blank sample, small amount of PFOA detected.

230412_PFAS-første_analyse009 Smooth(SG,3x3)
Standard1-6

MRM of 3 channels,ES-
413 > 369
5.009e+005

Perfluorooctanoic acid
1.38
13054.06
508537
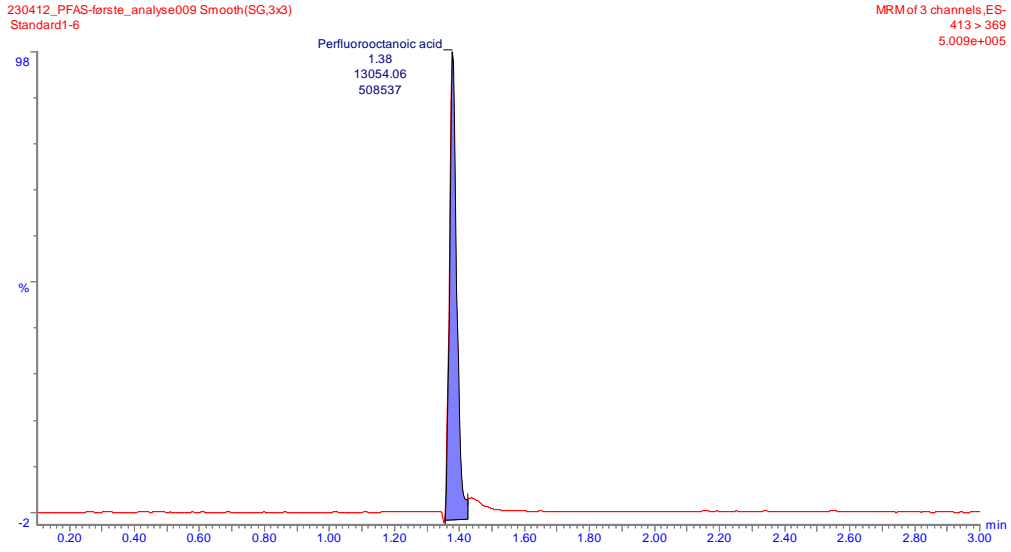
Figure A-9. PFOA detected, 0.1 mg/L.

230412_PFAS-første_analyse007 Smooth(SG,3x3)
Standard1-4

MRM of 3 channels,ES-
413 > 369
1.504e+005

Perfluorooctanoic acid
1.38
3666.83
150158*
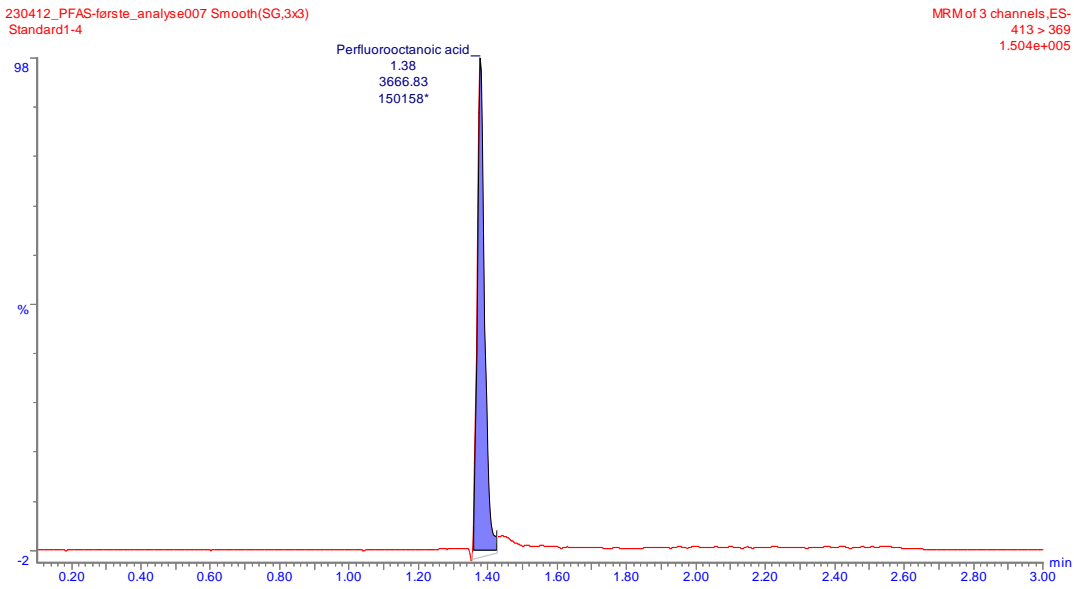
Figure A-10. PFOA detected, 0.03 mg/L.

230412_PFAS-første_analyse010 Smooth(SG,3x3)
Standard1-7

MRM of 3 channels,ES-
413 > 369
7.459e+005

Perfluorooctanoic acid
1.38
22680.72
762149
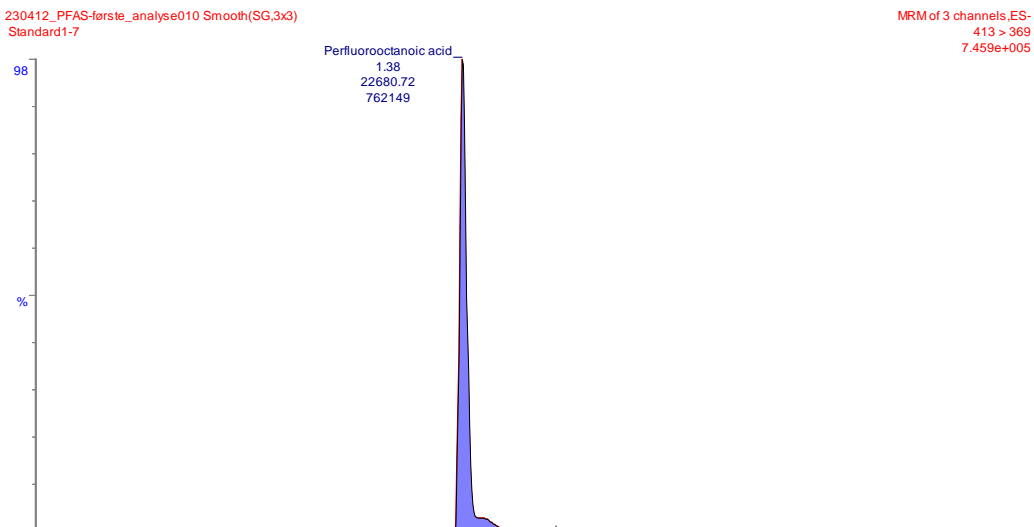
Figure A-11. PFOA detected, 0.15 mg/L.

1.30
8021.18
311142*
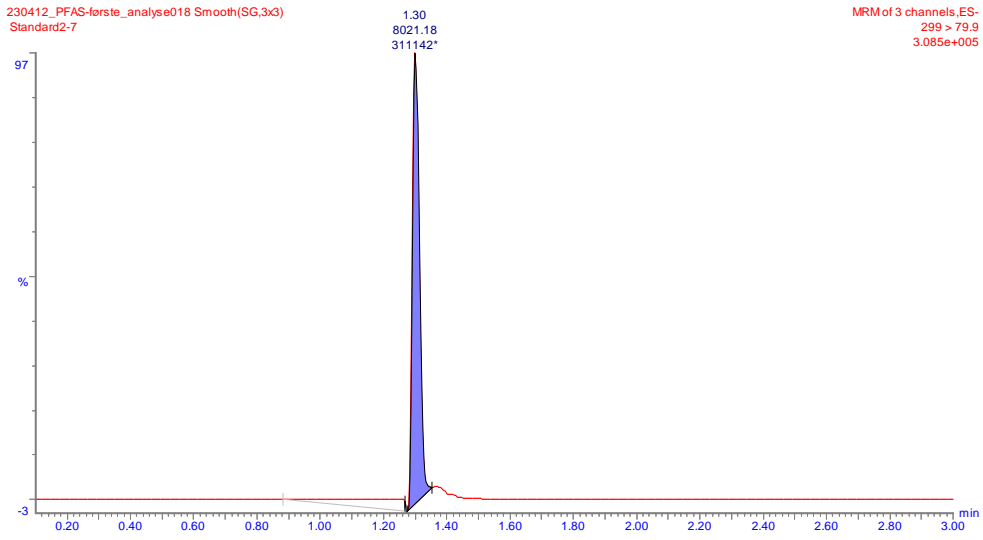
Figure A-12. PFBS detected, 0.15 mg/L.

1.30
10063.76
378866*
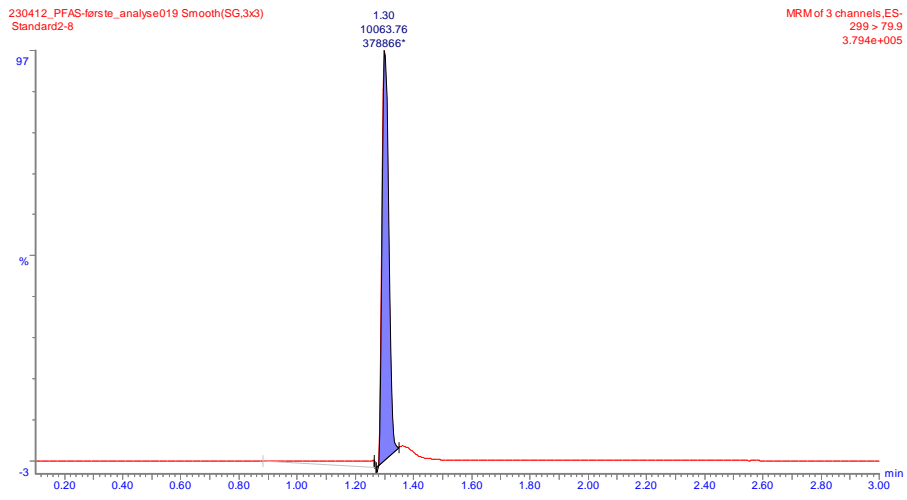
Figure A-13. PFBS detected, 0.20mg/L.
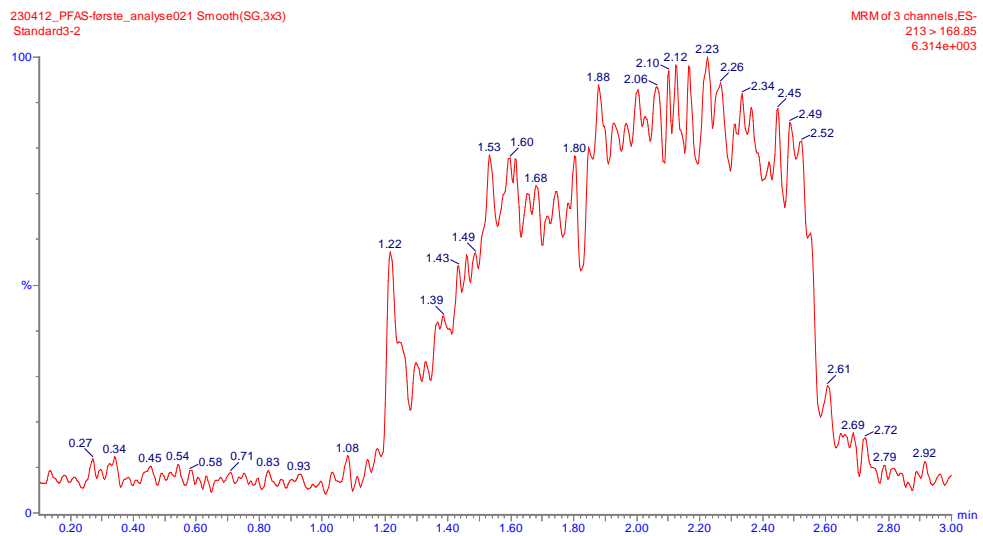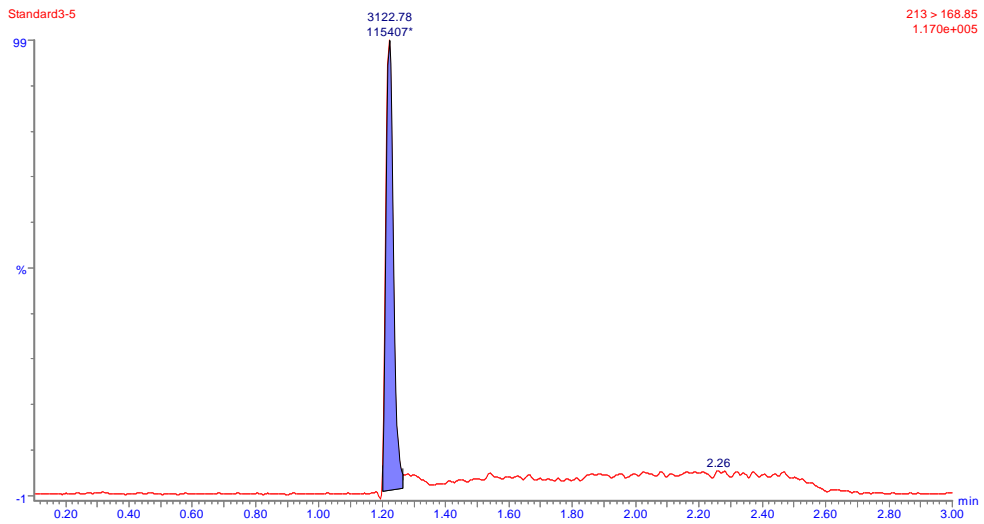
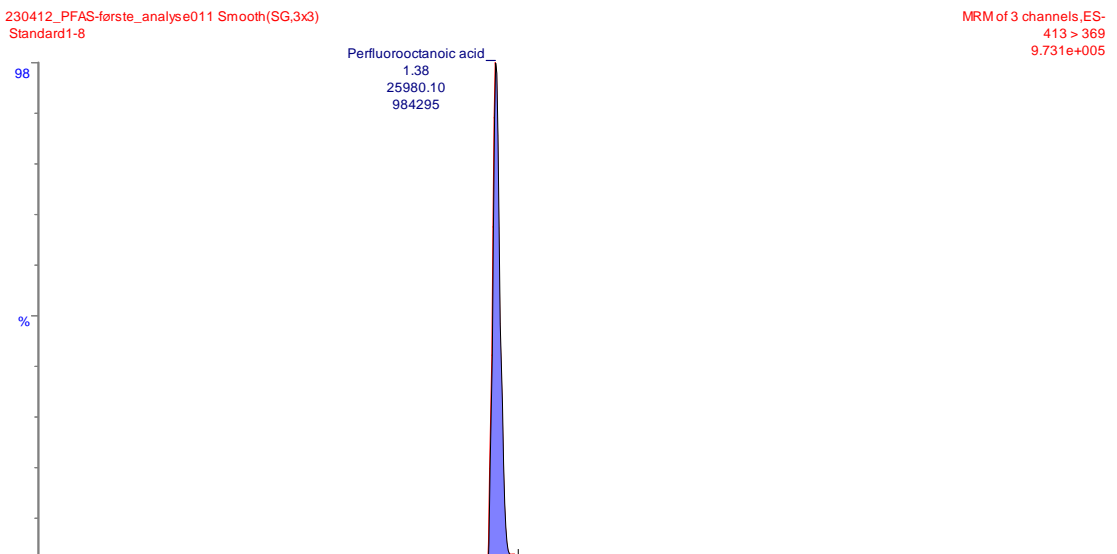*Figure A-14. No PFBA detected, 0.001 mg/L.*

54
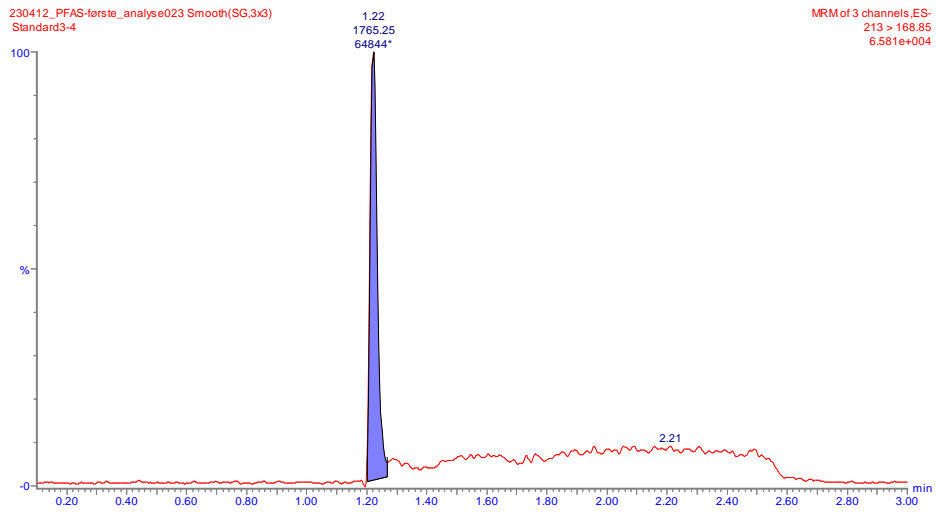
Figure A-15. PFBA detected, 0.03 mg/L.

Figure A-16. PFBA detected, 0.05 mg/L.

Figure A-17. PFOA detected, 0.0003 mg/L.

1.30
5402.54
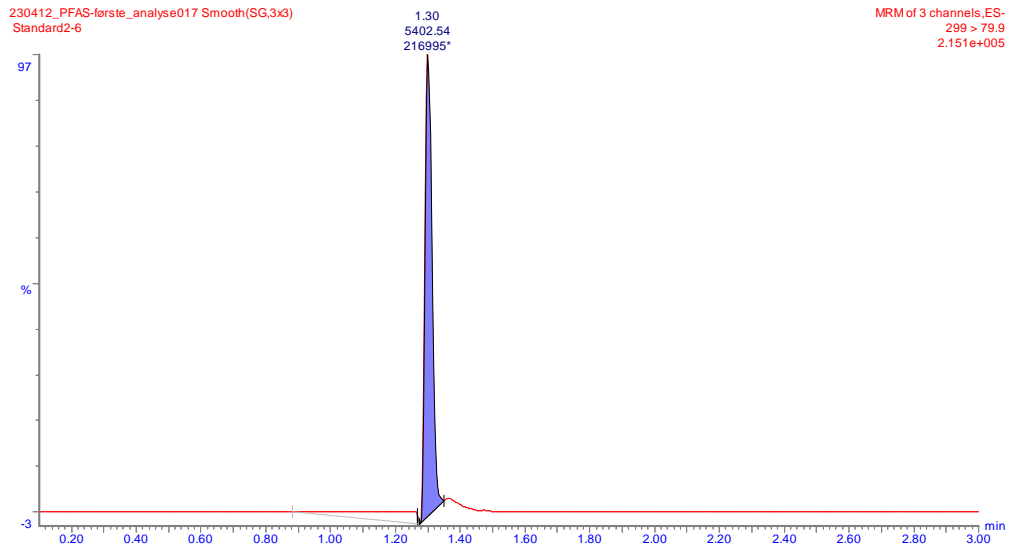216995*

MRM of 3 channels,ES-
299 > 79.9
2.151e+005

97

%

-3

0.20 0.40 0.60 0.80 1.00 1.20 1.40 1.60 1.80 2.00 2.20 2.40 2.60 2.80 3.00   min

Figure A-18. PFBS detected, 0.1 mg/L.

230412_PFAS-første_analyse013 Smooth(SG,3x3)
Standard2-2

1.30
60.85
2382*

MRM of 3 channels,ES-
299 > 79.9
2.362e+003

97

%

0.92

-3

0.20 0.40 0.60 0.80 1.00 1.20 1.40 1.60 1.80 2.00 2.20 2.40 2.60 2.80 3.00   min
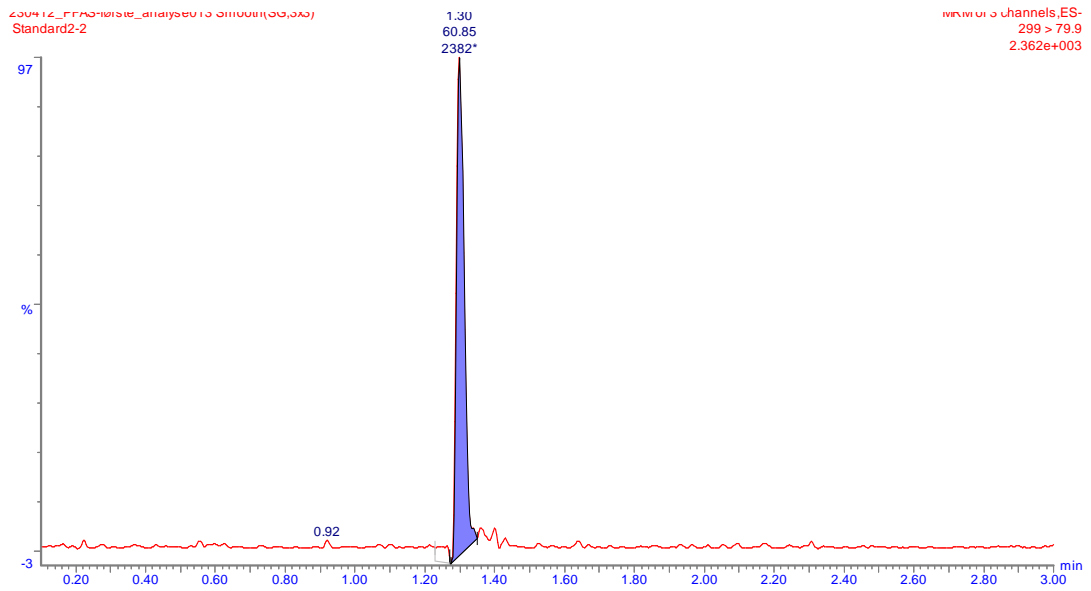
Figure A-19. PFBS detected, 0.001 mg/L.

Standard2-4

1.30
1677.17
66213*

299 > 79.9
6.552e+004

97

%

-3

0.20 0.40 0.60 0.80 1.00 1.20 1.40 1.60 1.80 2.00 2.20 2.40 2.60 2.80 3.00   min
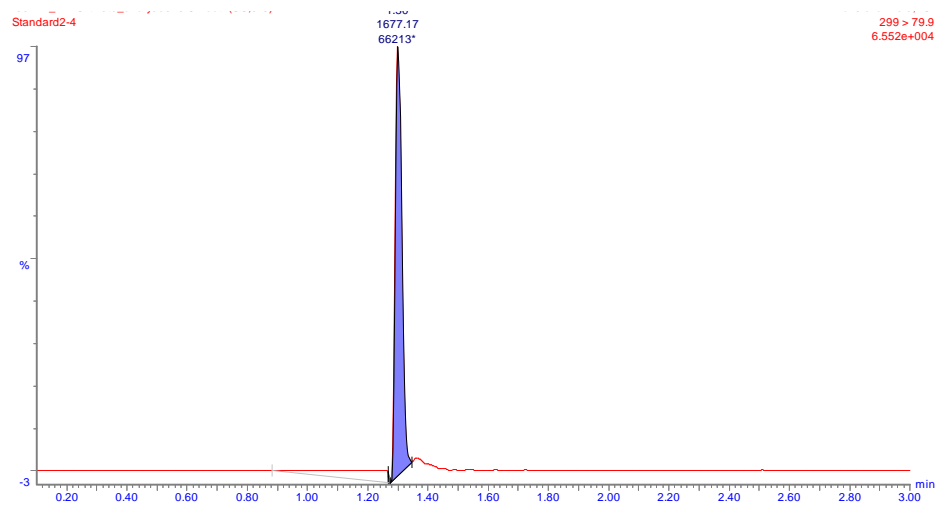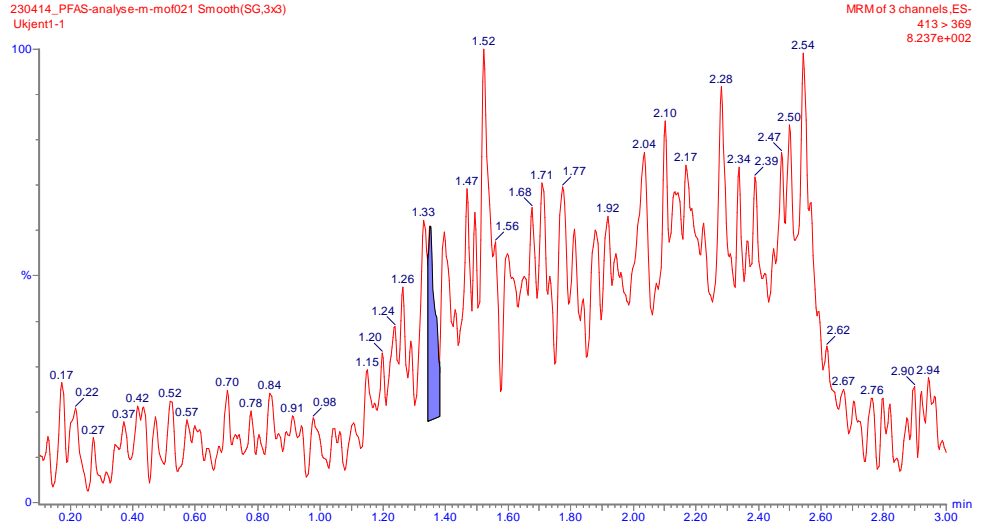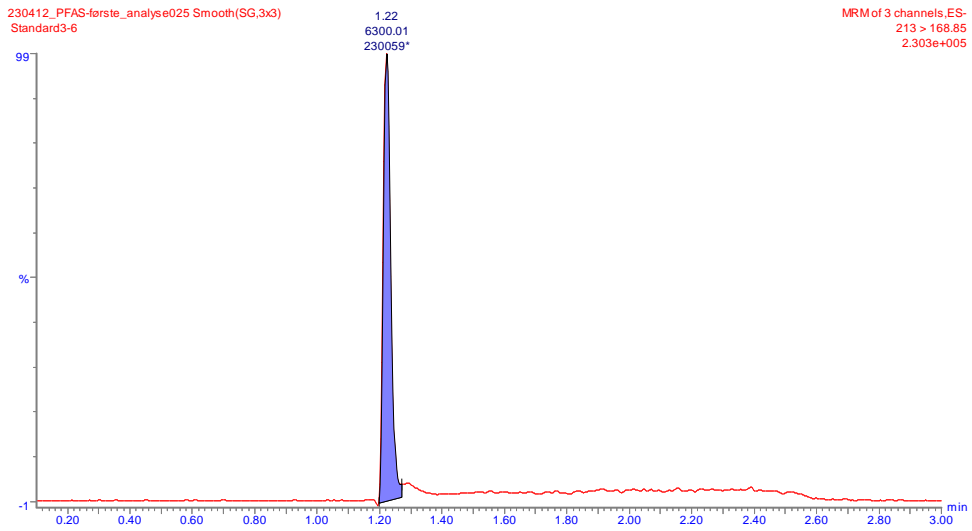
Figure A-20. PFBS detected, 0.03 mg/L.

Figure A-21. Unknown 1-1. No PFOA detected, 100% adsorption efficiency.
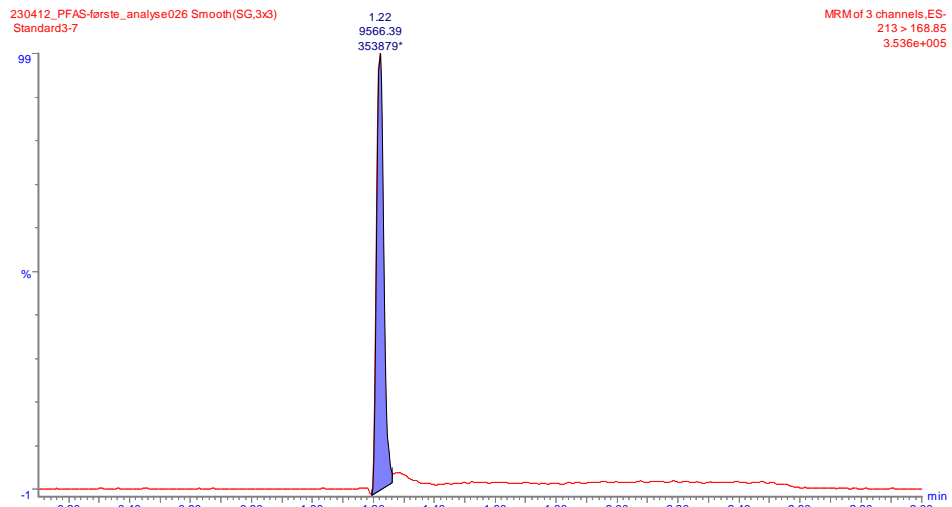

Figure A-22. PFBA detected, 0.1 mg/L.
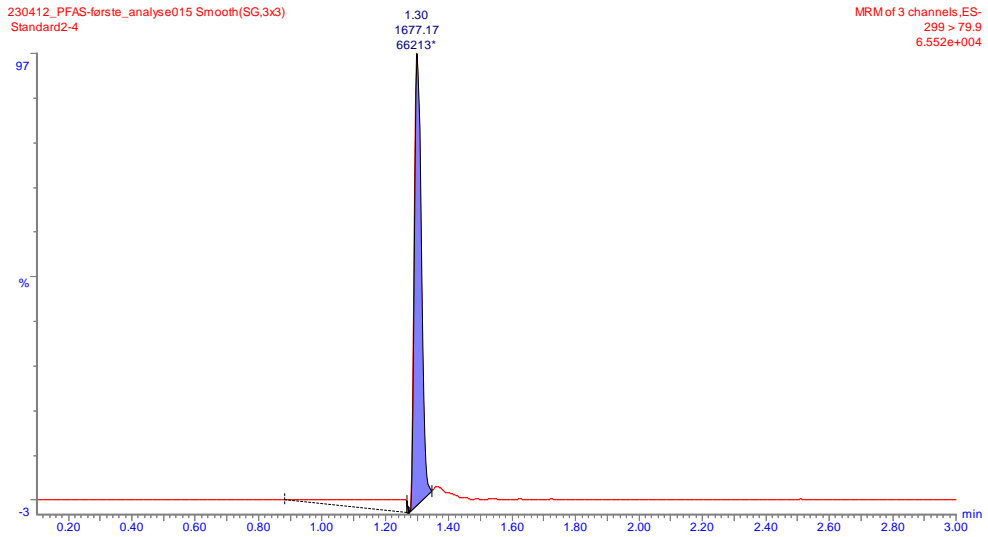

Figure A-23. PFBA detected, 0.15 mg/L.

230412_PFAS-første_analyse015 Smooth(SG,3x3)
Standard2-4

1.30
1677.17
66213*

MRM of 3 channels,ES-
299 > 79.9
6.552e+004

Figure A-24. PFBS detected, 0.03 mg/L.

230412_PFAS-første_analyse016 Smooth(SG,3x3)
Standard2-5

1.30
3213.20
130417*

MRM of 3 channels,ES-
299 > 79.9
1.296e+005
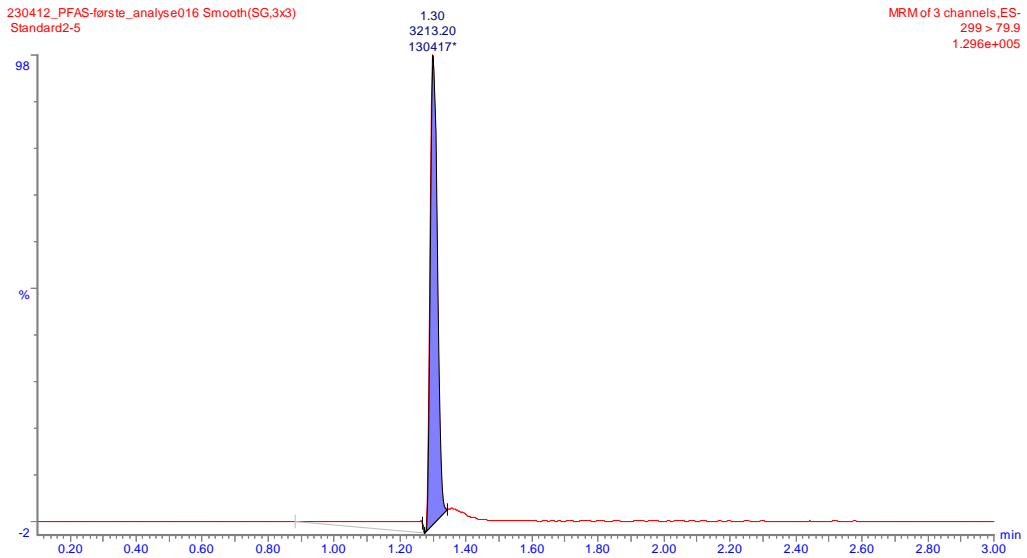
Figure A-25. PFBS detected, 0.05 mg/L.

230412_PFAS-første_analyse028 Smooth(SG,3x3)
Ukjent1

Perfluorooctanoic acid
1.38
62025.69
2355899*

MRM of 3 channels,ES-
413 > 369
2.347e+006
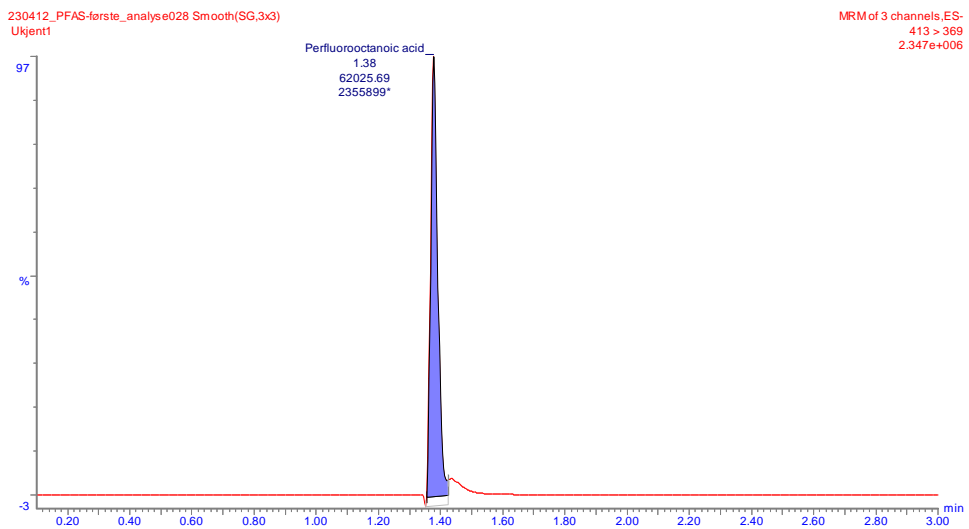
Figure A-26. Unknown sample, PFOA detected.

230412_PFAS-første_analyse027 Smooth(SG,3x3)
Standard3-8

1.22
12426.71
461045*

MRM of 3 channels,ES-
213 > 168.85
4.632e+005
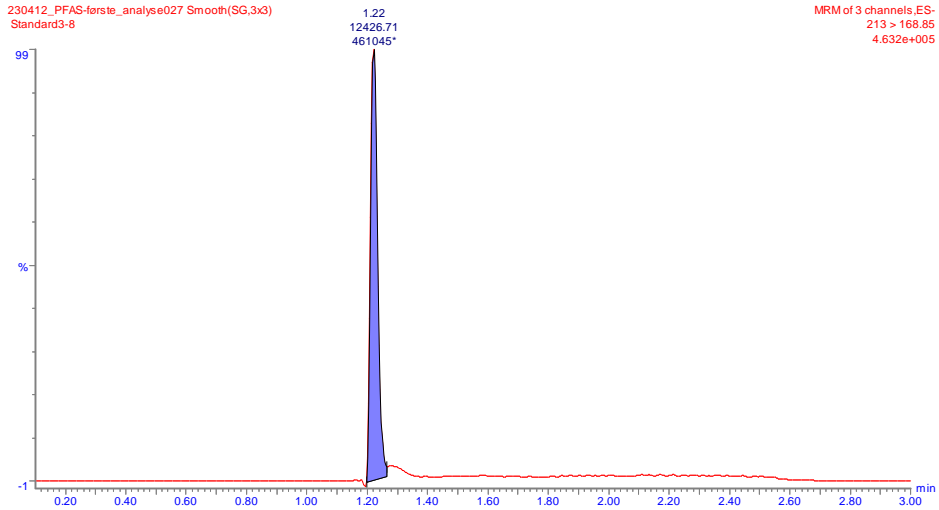
Figure A-27. PFBA detected, 0.20 mg/L

230412_PFAS-første_analyse029 Smooth(SG,3x3)
Ukjent2

Perfluorobutanesulfonic acid
1.30
64834.84
1819057*

MRM of 3 channels,ES-
299 > 79.9
1.834e+006
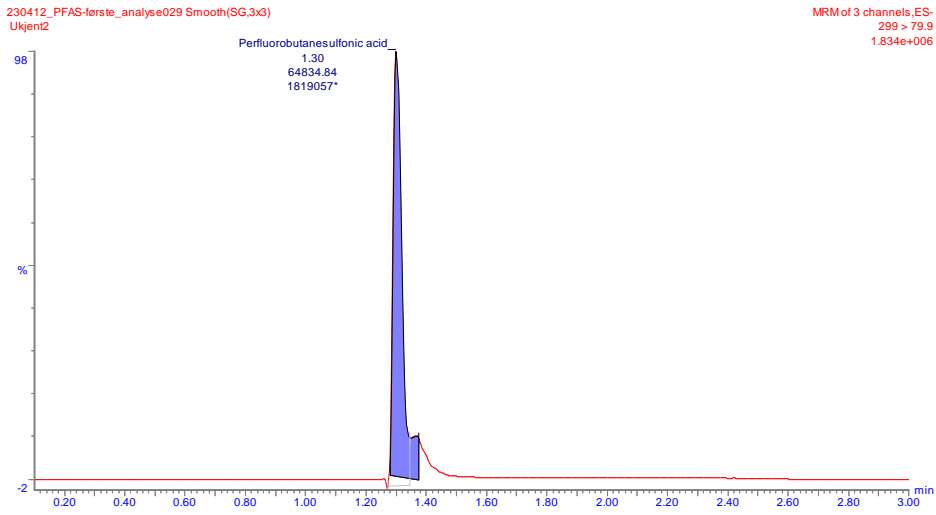
Figure A-28. Unknown, PFBS detected.

230412_PFAS-første_analyse030 Smooth(SG,3x3)
Ukjent3

1.22
187929.30
4207210*
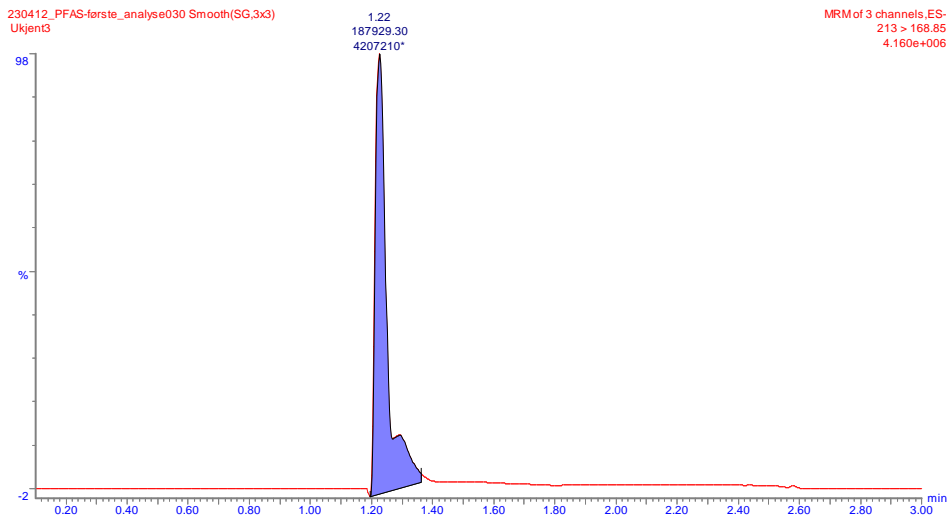
MRM of 3 channels,ES-
213 > 168.85
4.160e+006

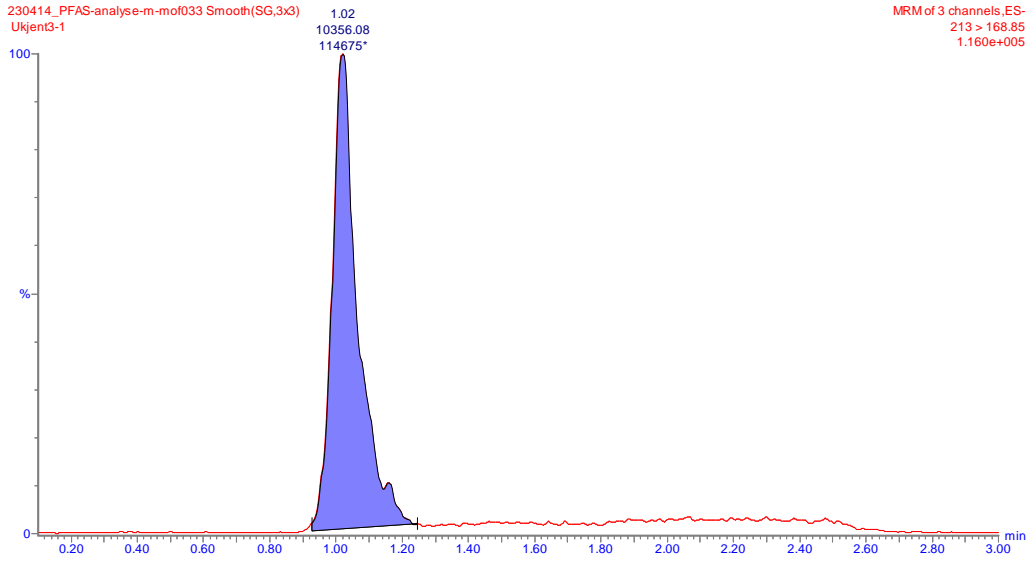*Figure A-29. Unknown, PFBA detected.*

59

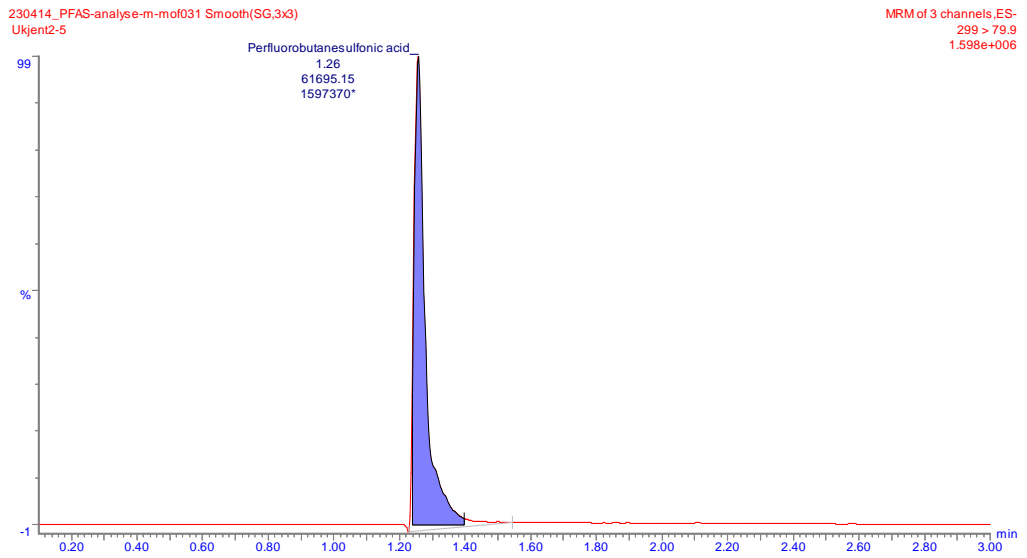*Figure A-30. Unknown sample, PFBA detected. Initial concentration was 0.2 mg/L.*

Figure A-31. Unknown sample, PFBS detected. Initial concentration was 6 mg/L.

Perfluorobutanesulfonic acid
1.26
92192.30
2148280*

Figure A-32. Unknown sample, PFBS detected. Initial concentration was 10 mg/L.

Perfluorobutanesulfonic acid
1.26
8548.68
310376*
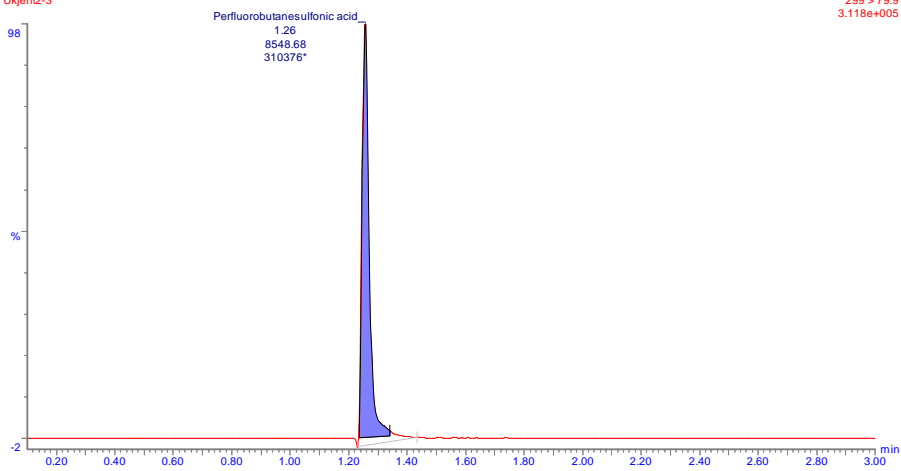
Figure A-33. Unknown sample, PFBS detected, Initial concentration was 0.8 mg/L.

Perfluorobutanesulfonic acid
1.25
7905.86
286495*

Figure A-34. Unknown sample, PFBS detected. Initial concentration was 0.5 mg/L

61

98

%

-2

Perfluorobutanesulfonic acid
1.25
85.43
3295*

0.48

0.20   0.40   0.60   0.80   1.00   1.20   1.40   1.60   1.80   2.00   2.20   2.40   2.60   2.80   3.00   min

Figure A-35. Unknown sample, PFBS detected. Initial concentration was 0.2 mg/L.

100

%

0

Perfluorobutanesulfonic acid
1.30
5.21
206

0.14   0.22
0.44   0.50   0.56
0.66
0.81   0.90
1.07   1.13   1.23
1.43   1.48   1.56
1.67
1.74   1.82
1.96   2.03
2.14   2.18
2.39   2.41
2.51   2.63   2.74   2.81   2.94

0.20   0.40   0.60   0.80   1.00   1.20   1.40   1.60   1.80   2.00   2.20   2.40   2.60   2.80   3.00   min

Figure A-36. Unknown sample, PFBA detected.

Perfluorooctanoic acid
1.33
24962.77
878449*

Figure A-37. Unknown sample, PFOA detected. Initial concentration was 10 mg/L.

1.01
80458.11
738997*

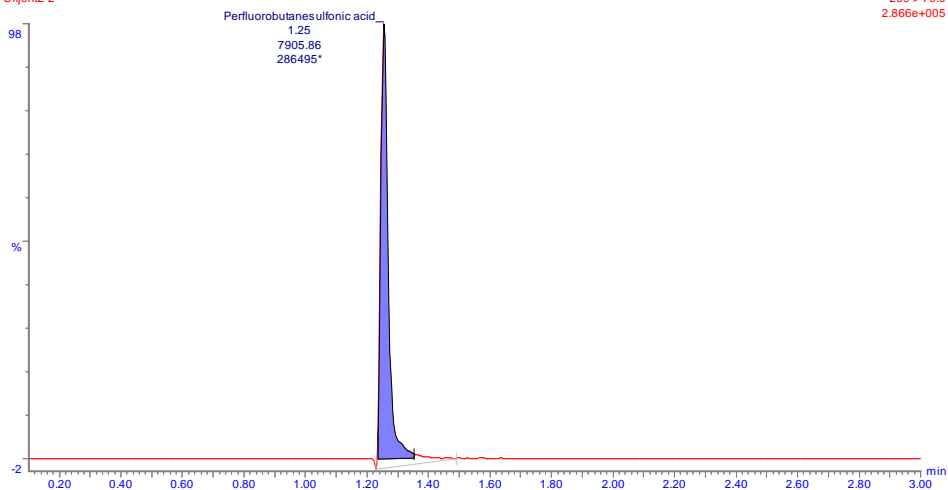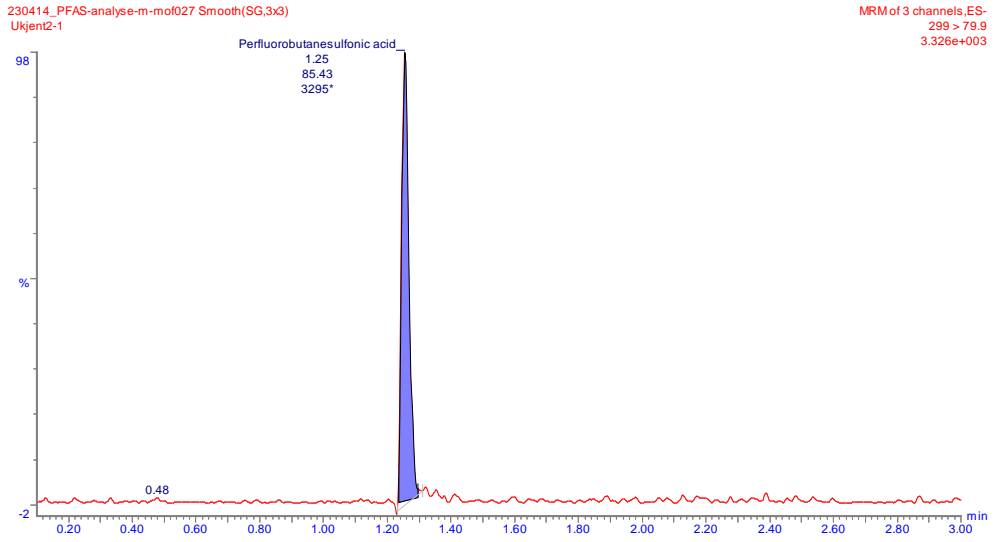*Figure A-38. Unknown sample, PFBA detected. Initial concentration was 2 mg/L.*

Figure A-39. Unknown sample, PFBA detected. Initial concentration was 0.5 mg/L.

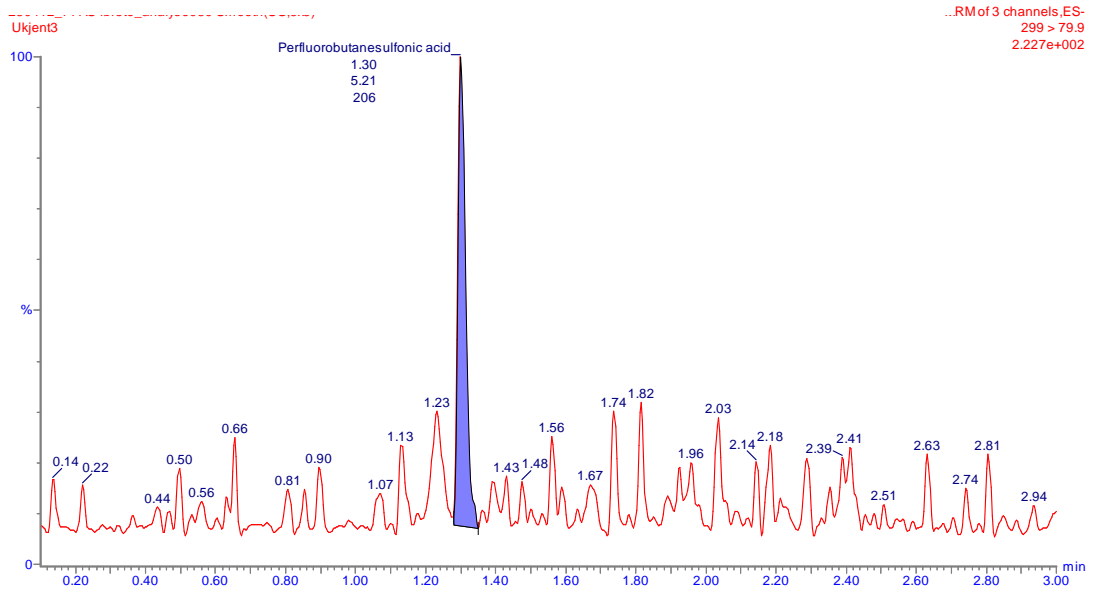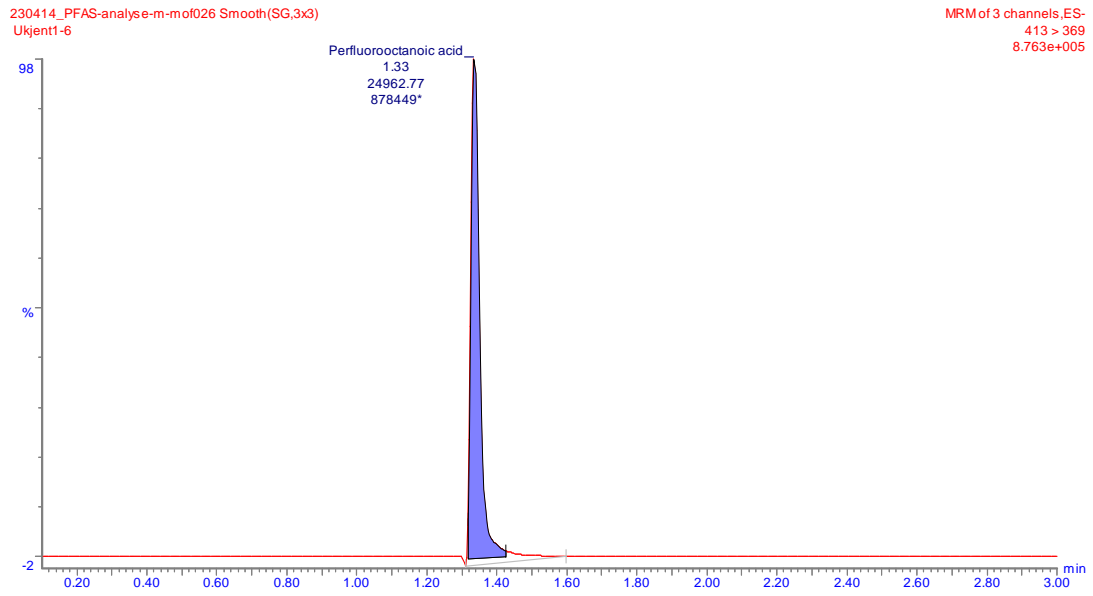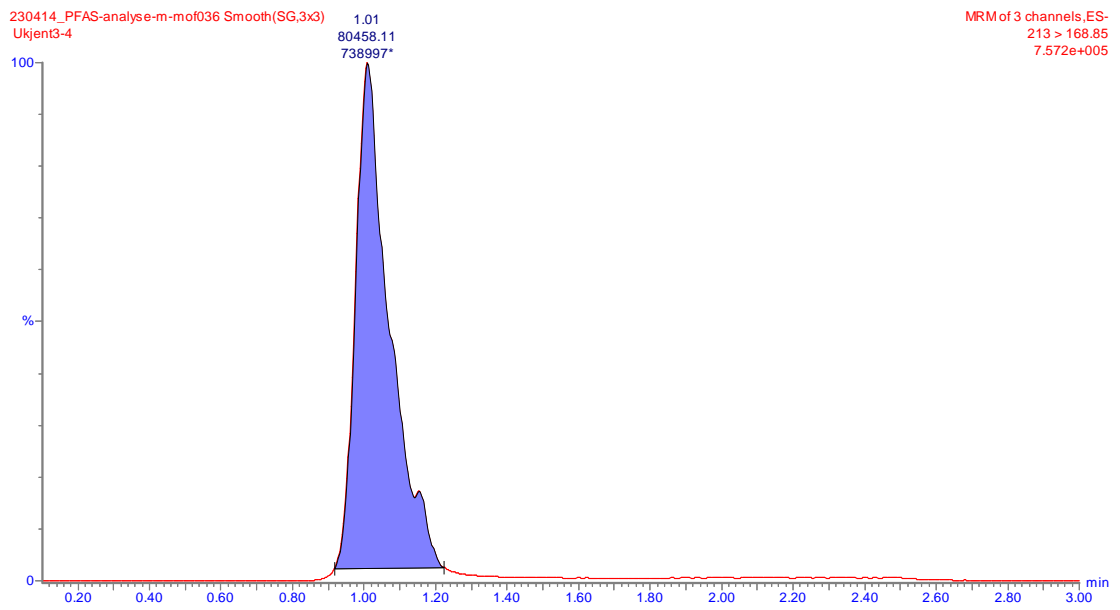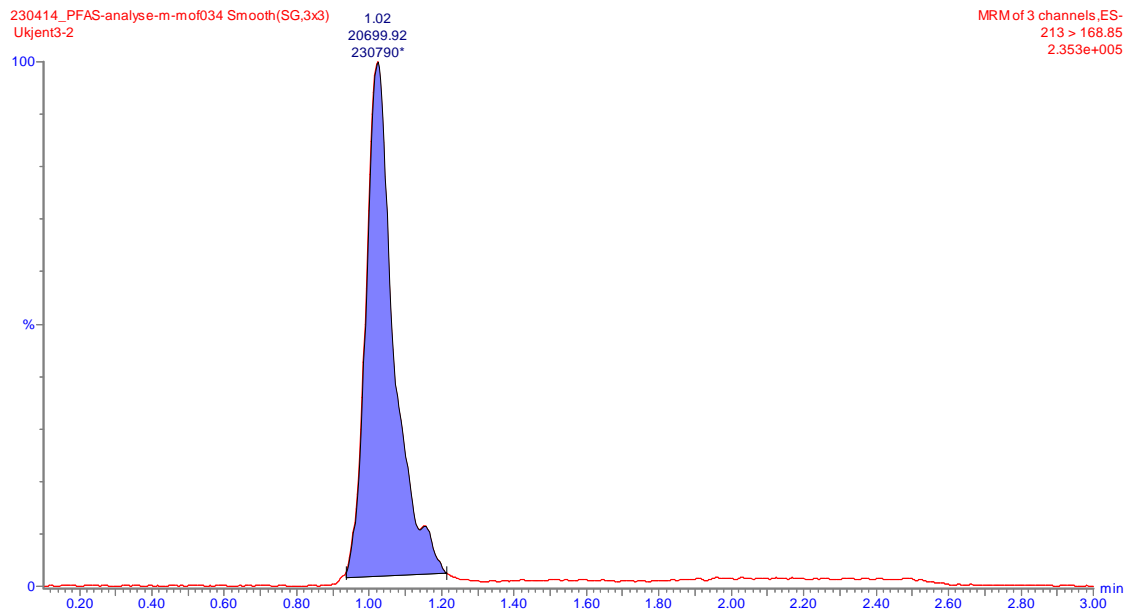*Figure A-40. Unknown sample, PFBS detected. Initial concentration was 2 mg/L.*
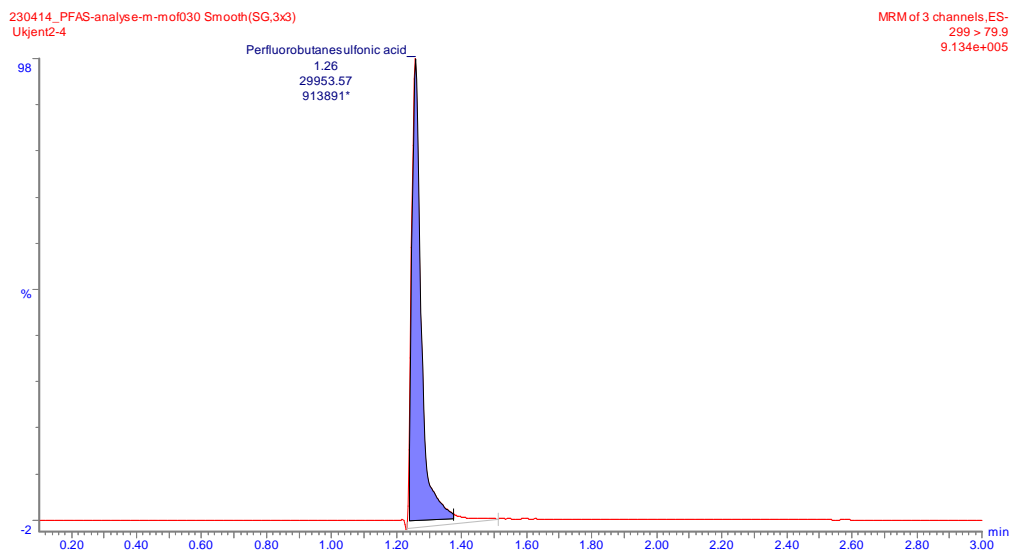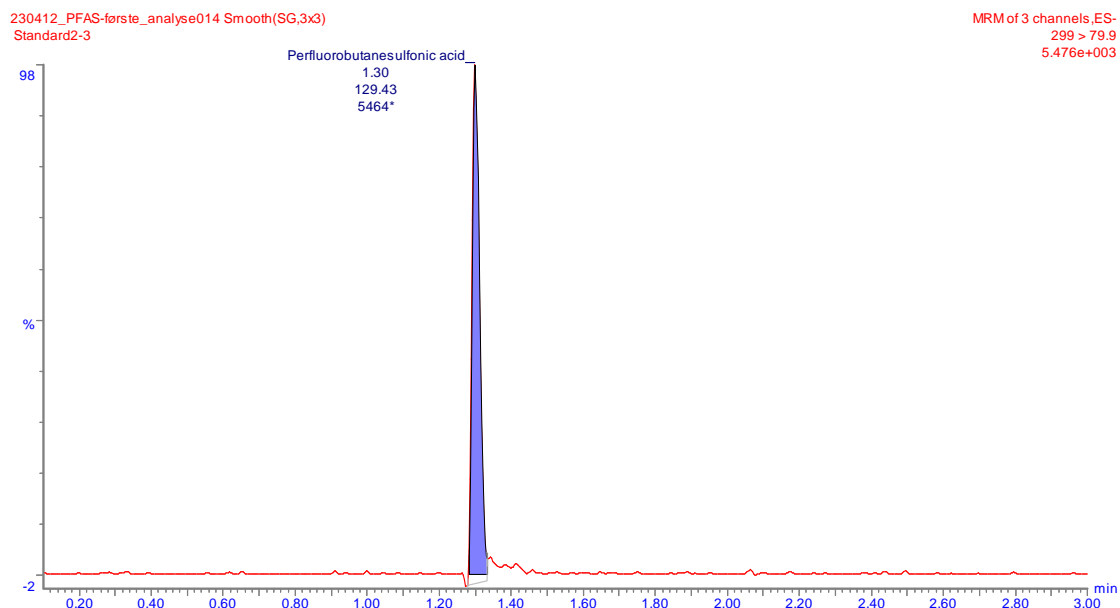
Perfluorobutanesulfonic acid
1.30
129.43
5464*

Figure A-41. Unknown sample, PFBS detected. Initial concentration was 0.8 mg/L.
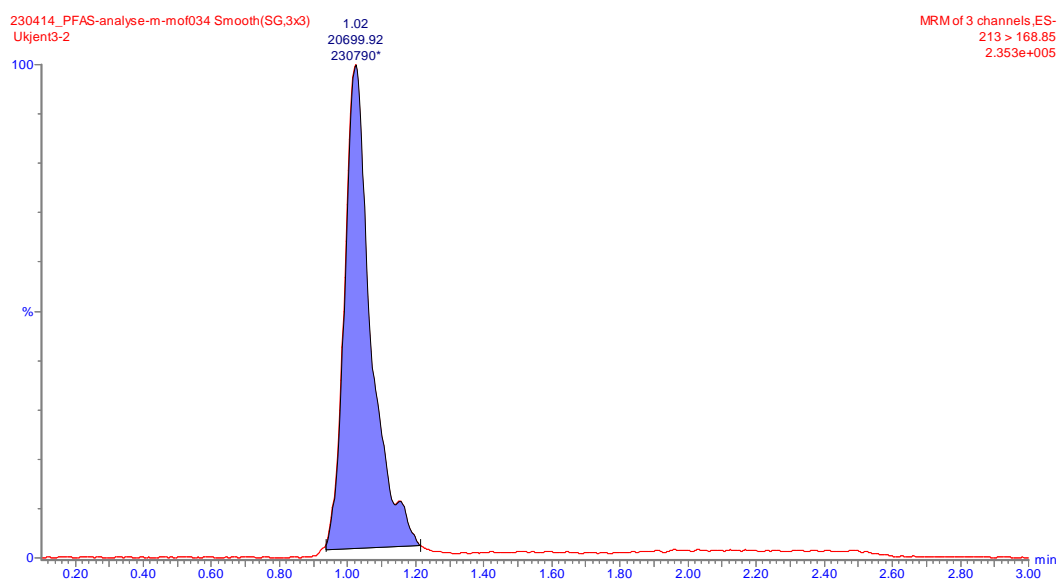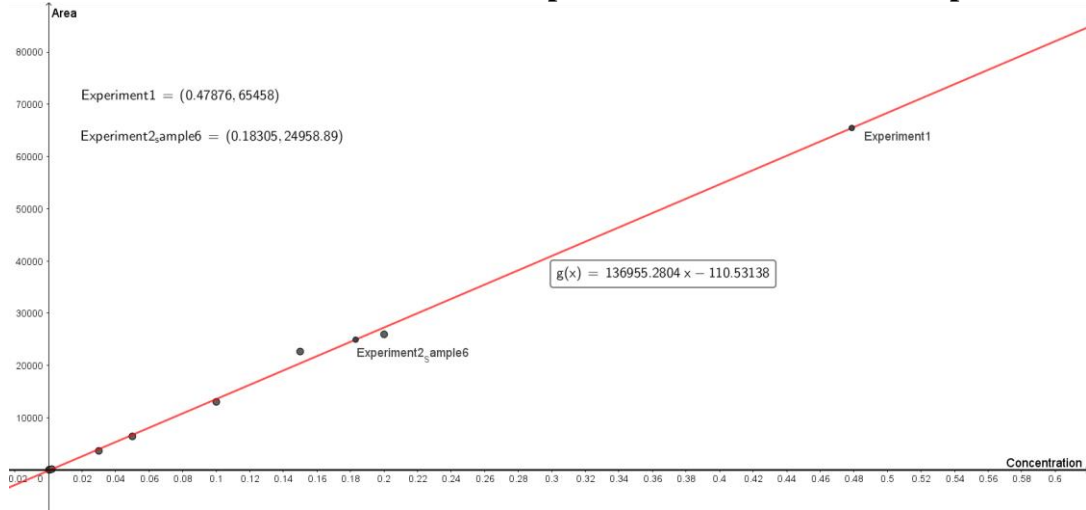
1.02
20699.92
230790*

Figure A-42. Unknown sample, PFBA detected. Initial concentration was 0.5 mg/L.

Calibration curves for each PFAS with points used to calculate adsorption efficiency:

Experiment1 = (0.47876, 65458)

Experiment2$_s$ample6 = (0.18305, 24958.89)

$g(x) = 136955.2804\,x - 110.53138$

Figur A-43. Calibration curve for PFOA with points for calculation adsorption efficiency.

Experiment2$_s$ample6 = (9.63568, 92303.27)

Experiment2$_s$ample5 = (6.59853, 63244.09)

Experiment2$_s$ample4 = (3.11538, 29917.59)

Experiment2$_s$ample3 = (0.89845, 8706.22)

Experiment2$_s$ample2 = (0.81866, 7942.78)

Experiment1$_s$ample2 = (6.53425, 62629)

$g(x) = 9567.91157\,x + 109.89067$
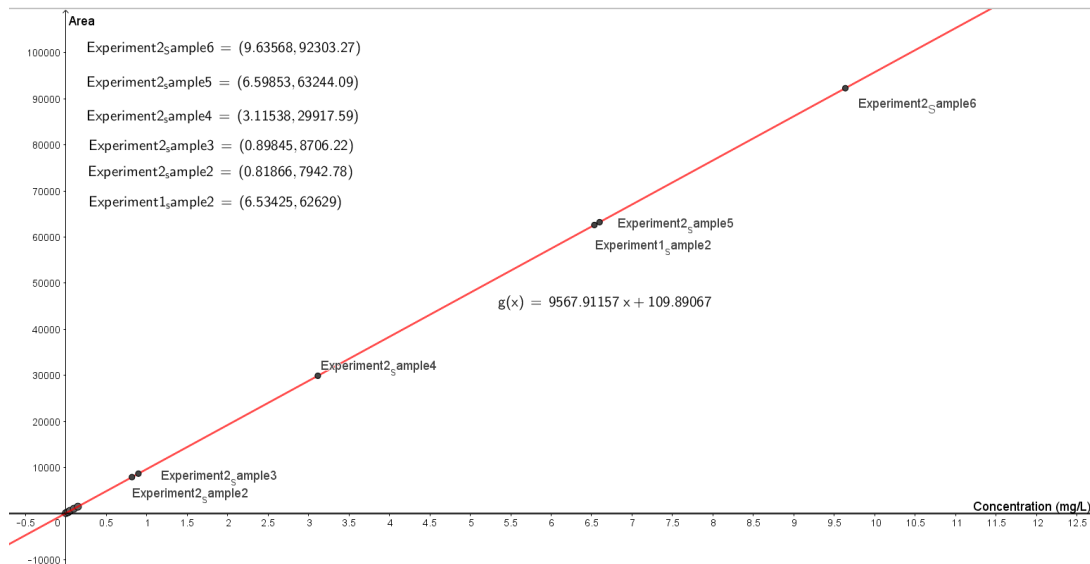
Figure A-44. Calibration curve for PFBS with points for calculation adsorption efficiency.

Experiment1$_s$ample1 = (2.56779, 151866.25)

Experiment2$_s$ample3 = (0.17299, 10306.35)

Experiment2$_s$ample4 = (0.35196, 20885.17)

Experiment2$_s$ample5 = (0.94064, 55682.93)

Experiment2$_s$ample6 = (1.38716, 82077.41)

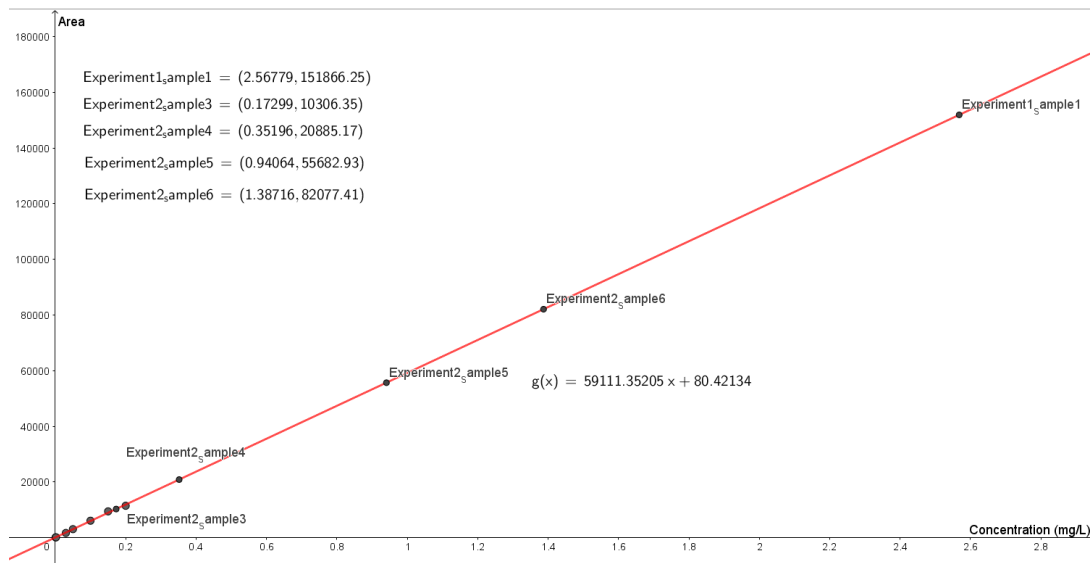$g(x) = 59111.35205\,x + 80.42134$

Figure A-45. Calibration curve for PFBA with points for calculation adsorption efficiency.

Tables for initial concentration, area, and concentration after adsorption:

Tabell A-1. Adsorption experiments for PFOA. Initial concentration, area of peak and concentration after adsorption for PFOA.

Sample nr:	Initial concentration:	Area:	Concentration after:
Experiment 1	10 mg/L	65458	0.47876mg/L
Experiment2_sample1	0.2 mg/l	Aprox. 0	Aprox. 0
Experiment2_sample2	0.5 mg/L	Aprox. 0	Aprox. 0
Experiment2_sample3	0.8 mg/L	Aprox. 0	Aprox. 0
Experiment2_sample4	2 mg/L	Aprox. 0	Aprox. 0
Experiment2_sample5	6 mg/L	Aprox. 0	Aprox. 0
Experiment2_sample6	10 mg/L	24958,89	0,18 mg/L

Tabell A-2. Adsorption experiments for PFBS. Initial concentration, area of peak and concentration after adsorption for PFBS.

Sample	Concentration before	Area	Concentration after
Experiment1_sample2	10 mg/L	62629	6.53
Experiment2_sample1	0.2 mg/L	Aprox. 0	Aprox. 0
Experiment2_sample2	0.5 mg/L	7942.78	0.8
Experiment2_sample3	0.8 mg/L	8706.22	0.89
Experiment2_sample4	2 mg/L	28817.59	3.11
Experiment2_sample5	6 mg/L	63244.09	6.60
Experiment2_sample6	10 mg/L	92303.27	9.64

Tabell A-3. Adsorption experiments for PFBA. Initial concentration, area of peak and concentration after adsorption for PFBA.

Sample	Concentration before	Area	Concentration after
Experiment1_sample1	10 mg/100ml	151866.25	2.56 mg /L
Experiment2_sample1	Not analyzed	-	-
Experiment2_sample2	Not analyzed	-	-
Experiment2_sample3	0.8 mg/L	10306.35	0.17
Experiment2_sample4	2 mg/L	20885.17	0.35
Experiment2_sample5	6 mg/L	55682.93	0.94
Experiment2_sample6	10 mg/L	82077.41	1.39